

1 THE TRANSITION FROM MIASKITIC TO AGPAITIC ROCKS AS MARKED BY THE  
2 ACCESSORY MINERAL ASSEMBLAGES, IN THE PASSA QUATRO ALKALINE  
3 COMPLEX (SOUTHEASTERN BRAZIL)

6 VINCENZA GUARINO<sup>§</sup>, ROBERTO DE' GENNARO, AND LEONE MELLUSO

*8 Dipartimento di Scienze della Terra, dell'Ambiente e delle Risorse, Università di Napoli Federico  
9 II, Complesso Universitario Monte Santangelo, Ed. L, Via Cintia 26, 80126 Naples, Italy*

EXCELSO RUBERTI, AND ROGÉRIO G. AZZONE

*Instituto de Geociências, Universidade de São Paulo, Rua do Lago 562, 05508-080 São Paulo, Brazil*

Brazil

21 RUNNING TITLE: Transition from miaskitic to agpaitic in the Passa Quattro complex

<sup>24</sup> § Corresponding author e-mail address: vincenza.guarino@unina.it

27 ABSTRACT

28

29 The Passa Quatro alkaline complex is one of the main intrusions found in the Serra do Mar  
30 Cretaceous to Paleogene Igneous Province. It is formed mainly by nepheline syenites and alkali  
31 syenites, with minor phonolitic dykes. The predominant felsic phases are alkali feldspar and  
32 nepheline, with very minor sodic plagioclase in less silica undersaturated rocks. The main mafic  
33 phases are clinopyroxene, amphibole, biotite and oxides. The wealth of accessory phases includes  
34 titanite, eudialyte, astrophyllite-kupletskite, F-disilicates, phosphates and silicophosphates, and F-  
35 REE- carbonates, with their specific ranges of composition. These accessory minerals often mantle  
36 corroded zircon (and fluorite) crystals, testifying the petrographic transition from miaskitic to  
37 agpaitic in the same rock. Looking at a regional scale, the three neighbouring complexes of Itatiaia,  
38 Passa Quatro and Poços de Caldas show similar mineral assemblages, but significant differences in  
39 the type of agpaitic minerals. The Passa Quatro intrusion (with aegirine, titanite and minor  
40 eudialyte) can be considered slightly more silica undersaturated and peralkaline than the nearby  
41 Itatiaia complex, and has transitional features towards the highly agpaitic nepheline syenites of  
42 Poços de Caldas (with aegirine, titanite, eudialyte and aenigmatite). Eudialyte and titanite represent  
43 the accessory phases able to influence the incompatible element behavior in the Serra do Mar  
44 potassic intrusive province.

45

46 **Keywords:** agpaitic, miaskitic, nepheline syenites, disilicates, Passa Quatro, Brazil

47

48

49 INTRODUCTION

50

51 The Mesozoic to Cenozoic alkaline magmatism of southern Brazil crops out in the central  
52 southeastern Brazilian Platform, close to Paraná Basin (Fig. 1a) and spans from ~132 to ~58 Ma,

with a peak at ~91-78 Ma (Morbidelli *et al.* 1995; Thompson *et al.* 1998; Guarino *et al.* 2013 and references therein). This magmatism has produced a large number of intrusive and sub-effusive complexes. Two important magmatic provinces are in southern Brazil, the Alto Paranaíba and Serra do Mar. The rocks belonging to these two provinces vary from strongly ultrabasic/ultramafic (carbonatites, kimberlites and kamafugites) to silicic in composition, showing mildly sodic to ultrapotassic affinity (Morbidelli *et al.* 1995; Thompson *et al.* 1998; Brotzu *et al.* 2005, 2007; Melluso *et al.* 2008, 2017; Azzone *et al.* 2009, 2013, 2016, 2017; Guarino *et al.* 2012, 2013, 2017; Gomes *et al.* 2011, 2017, 2018). In southernmost Brazil and Uruguay, the Cretaceous alkaline rocks (as Tunas, Cananéia, Piratini, Valle Chico/Mariscala) have mainly sodic affinity, with sporadic potassic and ultrapotassic compositions (Gomes *et al.* 2011; Morbidelli *et al.* 1995; Lustrino *et al.* 2005; Spinelli & Gomes 2008).

64 The Passa Quatro complex is an intrusive complex placed in the Serra do Mar Province. It is made  
65 up of mildly to strongly undersaturated syenites and nepheline syenites, and is crosscut by  
66 phonolitic dykes (Brotzu *et al.* 1992). The present paper aims to contribute to a better knowledge of  
67 type and composition of the accessory phases and their crystallization sequence and describe the  
68 evolution and enrichment conditions undergone by magmas to generate the Passa Quatro rocks.  
69 This study highlights the role that some accessory phases, such as titanite and eudialyte, have in the  
70 geochemical behavior of REE and HFSE in the intrusions of the Serra do Mar Province.

## GEOLOGICAL SETTING AND AGES

The Passa Quatro intrusive complex (Brotzu *et al.* 1992), is located about 150 km west of Rio de Janeiro (Fig. 1b), close to the larger massif of Itatiaia (Brotzu *et al.* 1997; Melluso *et al.* 2017; Rosa & Ruberti 2018). It is emplaced into the Precambrian basement, represented by the metamorphic complexes of Juiz de Fora, Paraíba do Sul and Açuengui Group (gneisses, migmatites, banded granulites, kinzigites, basic amphibolites; Hasui & Oliveira 1984). The field relationships with host

79 rocks are visible only in a few places, due to a large detrital talus and heavy forestation. Like the  
80 Itatiaia massif, Passa Quatro is structurally linked to the SE-Brazilian continental rift, along the  
81 Cabo Frio Magmatic Lineament (Riccomini *et al.* 2005 and references therein; Ferroni *et al.* 2018),  
82 developed into the Ribeira folded belt in an ENE to EW transcurrent system at the end of the  
83 Brasiliano cycle, and reactivated in connection with the Gondwana breakup (*e.g.*, Ribeiro *et al.*  
84 2018, and references therein). The Passa Quatro complex shows a subcircular shape, and covers an  
85 area of approximately 148 km<sup>2</sup>; geological mapping and cross-cutting field relationships suggest  
86 that it is made up of several distinct "ring-like" and "plug-like" bodies; however, post-emplacement  
87 normal SW- and SE-trending tectonics of Cenozoic age (Sigolo 1988), widespread in the southern  
88 part of the complex, and poor exposure and extensive weathering, preclude a better knowledge of  
89 the emplacement order of different magma pulses. A K-Ar age of  $66.7 \pm 3.3$  Ma (Ribeiro Filho &  
90 Cordani 1966, recalculated by Sonoki & Garda 1988) and the whole-rock Rb-Sr age of  $77 \pm 3$  Ma  
91 (Brotzu *et al.* 1992) were reported for the Passa Quatro rocks. These values are close to the more  
92 precise new U-Pb SHRIMP zircon ages reported by Rosa & Ruberti (2018) for the nearby Itatiaia  
93 massif, which comprises a range of 67.5-71 Ma, with indication for decreasing ages towards NW.  
94 This age interval is also similar to the K-Ar age of the age spread of the nearby Morro Redondo  
95 alkaline massif:  $67.2 \pm 4$  Ma (Ribeiro Filho & Cordani 1966, recalculated by Sonoki & Garda 1988)  
96 to  $\sim 73$  Ma (average age from determinations of Brotzu *et al.* 1989).

#### ANALYTICAL TECHNIQUES

100 The bulk-rock compositions are reported in Brotzu et al. (1992). The chemical composition of the  
101 main minerals (clinopyroxenes, feldspars, feldspathoids, amphiboles, micas and oxides) has been  
102 reported in Brotzu *et al.* (1992). In this study we report the chemical composition of the accessory  
103 minerals observed and identified in these rocks (Figs. 2 and 3; Suppl. Tab. A1). The chemical  
104 composition of mineral phases was determined on polished thin sections at Dipartimento di Scienze

105 della Terra, dell'Ambiente e delle Risorse (Di.S.T.A.R.), University of Napoli Federico II (a JEOL  
106 JSM-5310 microscope and an Oxford Instruments Microanalysis Unit, equipped with an INCA X-  
107 act detector and operating at 15 kV primary beam voltage, 50-100 mA filament current, variable  
108 spot size, from 30,000 to 200,000x magnification, 20 mm WD and 50 s net acquisition real time).  
109 Measurements were made with an INCA X-stream pulse processor and with INCA Energy  
110 software. Energy uses the XPP matrix correction scheme, developed by Pouchou & Pichoir (1988),  
111 and the Pulse Pile up correction. The quant optimization is carried out using cobalt (FWHM -full  
112 width at half maximum peak height- of the strobbed zero = 60-65 eV). The following standards,  
113 coming from Smithsonian Institute, were used for calibration: diopside (Ca), San Carlos olivine  
114 (Mg), anorthoclase (Al, Si), albite (Na), rutile (Ti), fayalite (Fe), Cr<sub>2</sub>O<sub>3</sub> (Cr), rhodonite (Mn),  
115 orthoclase (K), apatite (P), fluorite (F), barite (Ba), strontianite (Sr), zircon (Zr, Hf), synthetic  
116 Smithsonian orthophosphates (REE, Y, Sc), pure vanadium, niobium and tantalum (V, Nb, Ta),  
117 Corning glass (Th and U), sphalerite (S, Zn), sodium chloride (Cl), and pollucite (Cs). The K $\alpha$ , L $\alpha$ ,  
118 L $\beta$ , or M $\alpha$  lines were used for calibration, according to the element. Backscattered electron (BSE)  
119 images were obtained with the same instrument.  
120

## 121 CHEMISTRY AND PETROGRAPHY

122

123 The Passa Quattro alkaline rocks have a hypidiomorphic to slightly porphyritic structure, with  
124 coarse-grained texture (Fig. 2); sometimes they have cumulus or flow textures involving large alkali  
125 feldspar grains. These rocks are rich in alkali feldspar, while plagioclase is present in few samples.  
126 They contain variable amounts in nepheline, typically occurring with euhedral to subhedral shape or  
127 as interstitial phase. The mafic minerals are clinopyroxene, always present, amphibole, biotite and  
128 oxides. The main accessory minerals are titanite/eudialyte, astrophyllite-group minerals, F-  
129 disilicates, phosphates, silicophosphates and other Nb-Na-Mn-Zr-F-C-bearing accessory minerals.  
130 The rocks are nepheline syenites with minor phonolites and syenites according to the R<sub>1</sub>-R<sub>2</sub> diagram

131 (Fig. 1b). They have a peralkaline index [P.I. = molar (Na+K)/Al] ranging from 0.83-1.13,  
132 similarly to the trends of other Serra do Mar complexes (Fig. 1c). These rocks are characterized by  
133 relatively restricted major oxide variations, but with a very large range of trace element  
134 concentration, in agreement with the high variability in the mineralogical features of the interstitial  
135 phases (Brotzu *et al.* 1992). The chondrite-normalized REE patterns of the nepheline syenites are  
136 moderately fractionated (La<sub>N</sub>/Yb<sub>N</sub> from 14 to 44; the subscript “N” means chondrite-normalized  
137 values). Similarly to the other Serra do Mar nepheline syenites, the Passa Quatro rocks plot towards  
138 the phonolitic minimum in the Petrogeny Residua’s System (SiO<sub>2</sub>-nepheline-kalsilite) (Fig. 4).

139

140

## MINERAL CHEMISTRY

141

142 The crystal chemical formulas of main minerals identified in the Passa Quatro rocks are listed in  
143 Table 1.

144

145 *Main mineral phases*

146

147 Clinopyroxene is ubiquitous in the Passa Quatro rocks as phenocrysts and microlites in the  
148 groundmass of fine-grained lithotypes, and range in composition from salite to aegirine. They show  
149 variable composition in many chemical elements, as Mn (0.6-4.8 wt.% MnO), Na (1.7-13.7 wt.%  
150 Na<sub>2</sub>O), Fe (13.6-29.5 wt.% FeO), and Ti (0-4.0 wt.% TiO<sub>2</sub>). Aegirine is often rich in ZrO<sub>2</sub> (up to 3  
151 wt.%). Feldspar mostly has a perthitic structure, with exsolution lamellae of albite and orthoclase.  
152 Rare oligoclase has been found as rim of alkali feldspar crystals in syenites. The composition is  
153 mainly potassic, ranging in composition between anorthoclase to sanidine, and sometimes has  
154 orthoclase enrichment from core-to-rim. Feldspathoids are principally nepheline, with minor  
155 sodalite. Amphibole is widely present in these rocks as rims of salitic clinopyroxene, sometimes  
156 well developed around aegirine borders or as idiomorphic crystals in pyroxene-free assemblages.

157 Their composition is mostly hastingsite in non-peralkaline varieties, and rare arfvedsonite in  
158 peralkaline syenites. Amphibole is rich in MnO, from 3.1 to 5.2 wt.%. *Micas* are a sporadic phase in  
159 these rocks; they are Ti- or in Ti-Mn rich biotite (1.2-2.7 wt.% TiO<sub>2</sub>; 2.5-4.3 wt.% MnO). *Oxides*  
160 are ilmenite and Mn-rich magnetite (1-8.8 wt.% MnO).

161

162 *The composition of accessory mineral phases*

163

164 *Titanite* is a common accessory phase in nepheline syenites. It can be considered the main  
165 repository phase of HFSE and LREE (Table 2; Suppl. Tab. A2). The concentration of Nb<sub>2</sub>O<sub>5</sub> and  
166 ZrO<sub>2</sub> are variable from negligible to 8.4 wt.% and 3.7 wt.%, respectively. The highest concentration  
167 of Nb and Zr can be related to the substitution of Ti with Zr and Nb. The ΣREE<sub>2</sub>O<sub>3</sub> concentrations  
168 reach up to 5.3 wt.%. These compositions are observed in titanite in other alkaline rocks elsewhere  
169 (e.g., Wu *et al.* 2016, Melluso *et al.*, 2010, 2018).

170

171 *Eudialyte* is found in the phonolite PQ42 as crystals generally surrounded by F-disilicates and  
172 fluorite. It is a solid solution between different end-members. The predominant end-member  
173 components are oneillite (0.35-0.56 mol.%), kentbrooksite (0-0.56 mol.%), Ce-zirsilite (0-0.69  
174 mol.%) and eudialyte (0-0.29 mol.%) according to the classification proposed by Pfaff *et al.* (2010).  
175 The variability in the end-members highlights wide chemical variations in ΣREE<sub>2</sub>O<sub>3</sub> (2.8-7.5 wt.%),  
176 Nb<sub>2</sub>O<sub>5</sub> (0.4-3.3 wt.%), ZrO<sub>2</sub> (10.1-12.7 wt.%), MnO (4.4-7.4 wt.%) and SrO (0.2-1.2 wt.%) (Fig.  
177 5a; Table 2; Suppl. Tab. A3). A mineral with a composition of a kentbrooksite was also analyzed  
178 always in the phonolite PQ42. The wide chemical variation observed in the eudialyte minerals can  
179 be linked to several cationic substitutions, such as Si → Nb, Fe → Mn, (Ca, Na) → (REE, Sr) (e.g.,  
180 Johnsen *et al.* 2001).

181

182     *Astrophyllite-group minerals*. According to the nomenclature of Piilonen *et al.* (2003), astrophyllite  
183     and kupletskite are present at Passa Quatro (Fig. 5b; Table 2; Suppl. Tab. A4). The high F (up to  
184     2.02 *apfu*), moderate Zr (up to 0.56 *apfu*) and low Nb (up to 0.16 *apfu*) contents in both minerals  
185     suggest the following substitution  $Ti + F \leftrightarrow Zr + (F, OH)$  (Piilonen *et al.* 2003). The astrophyllite  
186     compositions are very similar to those described at Ilímaussaq (South Greenland; Macdonald *et al.*  
187     2007; Fig. 5b) and Junguni (Malawi; Woolley & Platt 1988).

188

189     *F-disilicates*. The main types of F-disilicates in the Passa Quatro rocks, following the compositional  
190     ordering proposed by Melluso *et al.* (2014, 2017 and references therein), are rinkite, rosenbuschite,  
191     hiortdahlite, wöhlerite, lävenite and Mn-bearing lävenite (Fig. 6a; Table 3; Suppl. Tab. A5). These  
192     crystals show a different position in the groundmass of these rocks; sometimes they form plate-  
193     shaped crystals, or intergrown between them, or have an interstitial position (Fig. 3). These F-  
194     disilicates can be barely defined by a single composition; rather, they represent discrete phases  
195     following a chemical solution of different end-members in the cuspidine – janhaugite series (Fig.  
196     6a). Rosenbuschite is analyzed in sample PQ40A; lävenite is found in samples PQ10 and PQ12.  
197     The other samples instead show a variable presence of disilicates as rinkite and lävenite, and minor  
198     rosenbuschite in sample PQ39; wöhlerite and hiortdahlite in sample PQ41; lävenite and minor  
199     rosenbuschite in sample PQ42; hiortdahlite and minor wöhlerite in sample PQ6; and wöhlerite and  
200     minor lävenite and hiortdahlite in sample PQ12C. These minerals show a wide variability in their Zr  
201     concentration, very low in rinkite (up to 0.4 wt.%  $ZrO_2$ ), high and similar in rosenbuschite (12.1-  
202     14.8 wt.%  $ZrO_2$ ) and wöhlerite (12.8-14.3 wt.%  $ZrO_2$ ) and slightly higher in hiortdahlite (14.4-18.8  
203     wt.%  $ZrO_2$ ). On the other hand, the concentration of Zr in lävenite varies between 0.3 and 23.4  
204     wt.%  $ZrO_2$ , with negative correlation with Ti (1.9-19.7 wt.%  $TiO_2$ ). The Ti concentration is similar  
205     in rinkite (7.7-9.0 wt.%  $TiO_2$ ) and rosenbuschite (8.1-9.8 wt.%  $TiO_2$ ) and is very low in wöhlerite  
206     (0.8-2.4 wt.%  $TiO_2$ ) and hiortdahlite (0.8-1.6 wt.%  $TiO_2$ ). The Mn-bearing lävenite has slightly  
207     higher Mn concentration (9.9-15.5 wt.% in  $MnO$ ) than lävenite (6.8-12.0 wt.%  $MnO$ ). Mn-bearing

208 låvenite has also higher concentration of Zr (22.7-33.1 wt.% ZrO<sub>2</sub>) and low variation in Ti (1.0-5.1  
209 wt.% TiO<sub>2</sub>). Wöhlerite, hiortdahlite and rosenbuschite have similar Mn (2.0-5.0 wt.%, 2.3-3.7 wt.%  
210 and 3.2-4.6 wt.% MnO, respectively), whereas rinkite has very low Mn (0-0.7 wt.% MnO). The  
211 observed chemical substitutions in the Passa Quattro F-disilicates are related to the cationic  
212 substitutions in the same site, as Ca → Na, and Fe → Zr+Nb (Fig. 6b and 6c). The Ti/Fe → Mn  
213 substitution is thus observed in the Mn-bearing låvenites.

214

215 *Phosphates and silicophosphates.* Apatite in the Passa Quattro rocks is enriched in REE (6.3-20.2  
216 wt.% ΣREE<sub>2</sub>O<sub>3</sub>; Table 2; Suppl. Tab. A6). In these rocks the apatite coexists with britholite, which  
217 better includes the REE from the residual magma during crystallization. The ΣREE<sub>2</sub>O<sub>3</sub>  
218 concentrations of britholite increase up to 61.4 wt.%, with SiO<sub>2</sub> up to 21.6 wt.%. The typical  
219 substitution process for apatite and britholite is Ca+P → (L)REE+Si. These minerals have the same  
220 substitution mechanisms defined for Itatiaia complex (Melluso *et al.* 2017; Fig. 5c).

221

222 *Other minor accessory phases.* Other Nb-Na-Mn-Zr-F-C-bearing accessory phases are present in  
223 the Passa Quattro rocks, mainly in interstitial position (Suppl. Tab. A7). Zircon is a ubiquitous early  
224 phase in the syenites. It is present as relict crystals surrounded by F-disilicates (Fig. 3). Baddeleyite  
225 (ZrO<sub>2</sub>) is tiny crystals in sample PQ10. Garnet is analyzed in sample PQ19. It represents a solid  
226 solution of andradite (79.1-89.0 mol.%) and grossular (1.8-14.5 mol.%), with moderate  
227 concentration of Mn (1.7-2.0 wt.% MnO) (Locock 2008). Pyrochlore shows variable concentration  
228 of UO<sub>2</sub> (0.6-8.7 wt.%). Hydroxymanganopyrochlore is identified in sample PQ10, with its high Mn  
229 concentration (28.5-42.9 wt.% MnO). Catapleiite is a hydrous phase rich in sodium (9.9-11.9 wt.%  
230 Na<sub>2</sub>O) and zirconium (29.4-31.1 wt.% ZrO<sub>2</sub>), and present in many nepheline-syenites. Pectolite is  
231 also identified in nepheline syenites. Fluorite (CaF<sub>2</sub>) is a groundmass phase, crystallizes earlier than  
232 some silicates and together with F-disilicates (Fig. 3). Undefined REE fluorocarbonates and REE

233 carbonates are identified in the interstices. Sphalerite [Zn(Fe)S] and kalistroneite [ $K_2Sr(SO_4)_2$ ] are  
234 also identified.

235

236 DISCUSSION

237

238 *Crystallization of accessory phases in the Passa Quattro intrusion*

239

240 The Passa Quattro rocks plot in the thermal trough between trachytic and phonolitic minima in the  
241 nepheline–kalsilite–silica phase diagram, as expected from evolved rocks having sodic affinity and  
242 silica-undersaturated composition (Fig. 4), confirming relatively low *liquidus* temperatures and a  
243 trend towards the phonolitic minimum.

244 Microscopic observation, back-scattered electron images and electron microprobe analyses of  
245 mineral phases indicate that the main mineral assemblage is formed by clinopyroxene, alkali  
246 feldspar and nepheline, followed by plagioclase, amphibole, and several accessory phases. The  
247 fractional crystallization started with clinopyroxene and potassic alkali feldspar, whose removal  
248 drove the liquids towards Na-rich compositions, then (Zr-bearing) aegirine and feldspathoids  
249 (mainly nepheline) started to crystallize. Removal of these phases produced enrichment in the  
250 incompatible elements (*e.g.*, HFSE, REE) and fluorine  $\pm$  H<sub>2</sub>O and Cl in the liquids; therefore,  
251 zircon, magmatic titanite or eudialyte could crystallize. The titanite crystallizes after aegirine and  
252 magnetite; zircon and eudialyte crystallize before F-disilicates and fluorite. These enriched liquids  
253 started to crystallize also HFSE-, REE- and F-enriched mineral phases, as F-disilicates,  
254 astrophyllite-kupletskeite, pyrochlore and fluorite, but their crystallization sequence is not easy to be  
255 unequivocally defined. Hiortdahlite crystallized together with other F-disilicates, such as wöhlerite,  
256 and with fluorite and baddeleyite; lävenite probably crystallized after kupletskeite (and astrophyllite),  
257 or at least simultaneously. At the end of this crystallization path, the residual liquids begin to  
258 crystallize mineral phases containing CO<sub>2</sub> and H<sub>2</sub>O, as undefined REE carbonates, undefined REE

259 fluorocarbonates and hydroxy-manganopyrochlore that crystallize in a very late stage, while  
260 catapleiite and pectolite represent the latest post-magmatic phases (as also reported by Larsen  
261 2010). This crystallization scheme (Fig. 7) well describes the evolution and compositional changes  
262 undergone by magmas that have generated Passa Quatro rocks through extensive crystallization  
263 processes starting from mafic parental magmas (basanites and leucite-nephelinites). The  
264 crystallization of HFSE-, REE- and F-enriched phases and their cationic substitution [Ca →  
265 Na/Mn+Fe → Zr+Nb/Ti → Mn, Si → Nb/Fe → Mn/(Ca, Na) → (REE, Sr)] well reflect the  
266 compositional changes undergone by magmas during its differentiation. These identified cationic  
267 substitutions describe the chemical variations observed for the F-disilicates, which also represent  
268 the main variation defined during magma differentiation. So this mineral assemblage, following the  
269 enrichment in HFSEs, REEs, high F and minor CO<sub>2</sub> and H<sub>2</sub>O, represents the typical chemical  
270 feature of agpaitic magma in an environment at low oxygen fugacity, and related to temperature  
271 decrease. The chemical feature of magmas suggest also an ultimately high degree of enrichment in  
272 the metasomatized mantle sources (*e.g.*, Arzamastsev *et al.* 2001; Upton *et al.* 2003; Guarino *et al.*  
273 2013, 2017).

274

275 *Regional significance*

276

277 The typical agpaitic assemblage is defined by the presence of HFSE minerals such as eudialyte, F-  
278 disilicates, and aenigmatite (see Marks & Markl, 2017). In the Serra do Mar Province, three  
279 neighbouring complexes of Itatiaia, Passa Quatro and Poços de Caldas show significant differences  
280 in their agpaitic mineral assemblage. These complexes contain F-disilicates, fluorite and titanite as  
281 main minerals (*e.g.*, this study; Melluso *et al.* 2017; Brotzu *et al.* 1997; Ulbrich *et al.* 2002; Vlach *et*  
282 *al.* 2018). Eudialyte is present in the Passa Quatro and Poços de Caldas, aegirine is in the Passa  
283 Quatro and Itatiaia, while aegirine and aenigmatite are found at Poços de Caldas. The presence or  
284 absence of eudialyte and aenigmatite minerals are due to their relative stability field which depends

285 upon peralkalinity, silica activity ( $a_{\text{SiO}_2}$ ),  $f_{\text{O}_2}$ , and  $a_{\text{H}_2\text{O}}$  (e.g., Andersen & Sørensen 2005; Markl *et al.*  
286 2010; Marks *et al.* 2011; Marks & Markl 2017). Therefore, the Passa Quatro intrusion can be  
287 considered more silica undersaturated and peralkaline than the nearby Itatiaia complex, but has  
288 transitional feature towards the highly agpaitic nepheline syenites of Poços de Caldas (cf. Ulbrich *et*  
289 *al.* 2002).

290 Looking at a regional scale, the REE concentrations in syenitic/phonolitic rocks, exemplified in  
291 Figure 8, indicates a significantly similar geochemistry of REE in the alkaline complexes of Serra  
292 do Mar down. We note that most of the nepheline syenites (and phonolites) of the Serra do Mar  
293 province (Passa Quatro, Itatiaia, Morro Redondo, Morro de São João, Cabo Frio; Fig. 8) contain  
294 significant amounts of idiomorphic titanite in their mineral assemblages. Hence, even limited  
295 removal of titanite is to be taken into account in the petrogenetic models involving REE, given the  
296 elevated partition coefficients of the phase for middle REE (cf. Melluso *et al.* 2018 and references  
297 therein). Different is for Monte de Trigo dykes, where the eudialyte is the main mineral that may  
298 influence the REE pattern (Fig. 8), notwithstanding the presence of titanite. On the other hand,  
299 within the magmatic evolution of complexes having silica-oversaturated, evolved felsic rocks (e.g.,  
300 Valle Chico/Mariscal in Uruguay, Brandberg in Namibia, or also the silicic peralkaline rocks in the  
301 African Rift), removal of titanite is considered to be less important than removal of other accessory  
302 phases. The effects of significant removal of garnet are highlighted by the depletion of heavy REE  
303 (and Y) in the most evolved phonolites of the Piratini field, in southermost Brazil (Barbieri *et al.*  
304 1987). At the Amis peralkaline granite of Brandberg (Namibia; Schmitt *et al.* 2000), the extreme  
305 enrichment in HREE and the marked Eu trough cannot be the effect of removal of minor phases  
306 rich in HREE (e.g., zircon, garnet, xenotime), together with alkali feldspar, and so is for the Valle  
307 Chico intrusion, having granites and quartz syenites with chevkinite and monazite (Lustrino *et al.*  
308 2005 and authors' unpublished data).

309 The similarity of the late-stage evolution (with concave REE pattern) in the Passa Quatro nepheline  
310 syenites with that observed in volcanic sequences found elsewhere, even in different tectonic

311 settings, can be used to check the role of key accessory minerals. For example, the concave REE  
312 patterns of trachytes from Ischia island (Italy), trachytes and phonolites of Libya and Madagascar  
313 (Melluso *et al.* 2014, 2018; Lustrino *et al.* 2012; Cucciniello *et al.* 2016) and several other syenitic  
314 intrusions elsewhere, indicate that titanite removal is a widespread and significant petrogenetic  
315 process in highly evolved and oxidized alkaline magmas, and that exploitation of REE- and HFSE-  
316 bearing nepheline syenitic rocks is to be carefully linked to the establishment of the degree of  
317 magmatic evolution of the samples and with the presence (and removal) of titanite, plus other  
318 scavenging accessory phases.

319

## 320 CONCLUSIONS

321

322 The wide, variable and problematic relationships between mineral assemblages in the intrusive  
323 rocks of Passa Quatro testify complex conditions at the base of their formation. The crystallization  
324 sequence is justified by fractional crystallization processes from parental mafic magmas at low  
325 oxygen fugacity and high fluorine and chlorine activity. The Passa Quattro intrusion is, on the  
326 average, more silica undersaturated and peralkaline than the nearby Itatiaia complex, thus being  
327 transitional towards the highly agpaitic nepheline syenites of Poços de Caldas. The presence of  
328 noteworthy accessory phases, already described in the Serra do Mar alkaline Province, speak for the  
329 importance of crystallization of REE-rich phases, such as eudialyte and titanite to assume  
330 petrological importance to define the transition from miaskitic to agpaitic syenites, and then to  
331 highly agpaitic nepheline syenites.

332

## 333 ACKNOWLEDGEMENTS

334

335 The authors thank Pietro Brotzu, Celso Gomes, Vincenzo Morra and Michele Lustrino for their  
336 advice during the course of this study, and Sergio Bravi for the preparation of several polished thin

337 sections for the mineral chemical work. This manuscript has been supported by Ricerca  
338 Dipartimentale and MIUR 2015 (alkaline and peralkaline rocks in the Mediterranean area, grant  
339 20158A9CBM to L.M.).

340

341 REFERENCES

342

343 ANDERSEN, T. & SØRENSEN, H. (2005) Stability of naujakasite in hyperagpaitic melts, and the  
344 petrology of naujakasite lujavrite in the Ilímaussaq alkaline complex, South Greenland.  
345 *Mineralogical Magazine*, **69**, 125–136.

346 ANDERSEN, T., ERAMBERT, M., LARSEN, A.O., & SELBEKK, R.S. (2010) Petrology of nepheline  
347 syenite pegmatites in the Oslo Rift, Norway: zirconium silicate mineral assemblages as  
348 indicators of alkalinity and volatile fugacity in mildly agpaitic magmas. *Journal of Petrology*,  
349 **51**, 2303–2325.

350 ANDERSEN, T., ERAMBERT, M., LARSEN, A.O., & SELBEKK, R.S. (2012a) Petrology of nepheline  
351 syenite pegmatites in the Oslo Rift, Norway: Zr and Ti mineral assemblages in miaskitic and  
352 agpaitic pegmatites in the Larvik Plutonic Complex. *Mineralogia*, **44**, 61–98.

353 ANDERSEN, T., CARR, P., & ERAMBERT, M. (2012b) Late-magmatic mineral assemblages with  
354 siderite and zirconian pyroxene and amphibole in the anorogenic Mt Gibraltar microsyenite,  
355 New South Wales, Australia, and their petrological implications. *Lithos*, **151**, 46–56.

356 ARZAMASTSEV, A.A., BEA, F., GLAZNEV, V.N., ARZAMASTSEVA, L.V., & MONTERO P. (2001) Kola  
357 alkaline province in the Paleozoic: evaluation of primary mantle magma composition and  
358 magma generation conditions. *Russian Journal of Earth Sciences*, **3**, 1–32.

359 AZZONE, R.G., RUBERTI, E., DA SILVA, J.C.L., GOMES, C.B., ENRICH, G.E.R., DE HOLLANDA,  
360 M.H.B.M., & TASSINARI, C.C.G. (2017) Upper Cretaceous weakly to strongly silica-  
361 undersaturated alkaline dike series of the Mantiqueira Range, Serra do Mar alkaline province:

- 362 Crustal assimilation processes and mantle source signatures. *Brazilian Journal of Geology*,  
363 **48(2)**, 373–390.
- 364 AZZONE, R.G., MONTECINOS MUÑOZ, P., ENRICH, G.E.R., ALVES, A., RUBERTI, E., & GOMES, C.B.  
365 (2016) Petrographic, geochemical and isotopic evidence of crustal assimilation processes in the  
366 Ponte Nova alkaline mafic-ultramafic massif, SE Brazil. *Lithos*, **260**, 58–75.
- 367 AZZONE, R.G., ENRICH, G.E.R., GOMES, C.B., & RUBERTI, E. (2013) Trace element composition of  
368 parental magmas from mafic-ultramafic cumulates determined by in situ mineral analyses: the  
369 Juquiá mafic-ultramafic alkaline-carbonatite massif, SE Brazil. *Journal of South American Earth  
370 Sciences*, **41**, 5–21.
- 371 AZZONE, R.A., RUBERTI, E., ENRICH, G.E.R., & GOMES, C.B. (2009) Zr- and Ba-rich minerals from  
372 the Ponte Nova alkaline mafic-ultramafic massif, southeastern Brazil: indication of an enriched  
373 mantle source. *The Canadian Mineralogist*, **47**, 1087–1103.
- 374 BARBIERI, M., BECCALUVA, L., BROTZU, P., CONTE, A., GARBARINO, C., GOMES, C.B., LOSS, E.L.,  
375 MACCIOTTA, G., MORBIDELLI, L., SCHEIBE, L.F., TAMURA, R.M., & TRAVERSA, G. (1987)  
376 Petrological and geochemical studies of alkaline rocks from continental Brazil. 1. The phonolite  
377 suite from Piratini, R.S. *Geochimica Brasiliensis*, **1**, 109–138.
- 378 BROTZU, P., BECCALUVA, L., CONTE, A., FONSECA, M., GARBARINO, C., GOMES, C.B., LEONG R.,  
379 MACCIOTTA, G., MANSUR, R.L., MELLUSO, L., MORBIDELLI, L., RUBERTI, E., SIGOLO, J.B.,  
380 TRAVERSA, G., & VALENÇA, J.G. (1989) Petrological and geochemical studies of alkaline rocks  
381 from continental Brazil. 8. The syenitic intrusion of Morro Redondo, R.J. *Geochimica  
382 Brasiliensis*, **3**, 63–80.
- 383 BROTZU, P., BARBIERI, M., BECCALUVA, L., GARBARINO, C., GOMES, C.B., MACCIOTTA, G.,  
384 MELLUSO, L., MORBIDELLI, L., RUBERTI, E., SIGOLO, J.B., & TRAVERSA, G. (1992) Petrology and  
385 geochemistry of the Passa Quatro alkaline complex, southeastern Brazil. *Journal of South  
386 American Earth Sciences*, **6**, 237–252.

- 387 BROTZU, P., GOMES, C.B., MELLUSO, L., MORBIDELLI, L., MORRA, V., & RUBERTI, E. (1997)
- 388 Petrogenesis of coexisting SiO<sub>2</sub>-undersaturated to SiO<sub>2</sub>-oversaturated felsic igneous rocks: the
- 389 alkaline complex of Itatiaia, southeastern Brazil. *Lithos*, **40**, 133–156.
- 390 BROTZU, P., MELLUSO, L., D'AMELIO, F., & LISTRINO, M. (2005) Mafic/ultramafic dykes and felsic
- 391 intrusions with potassic to ultrapotassic affinity in the Serra do Mar province: a review. *In*
- 392 Mesozoic to Cenozoic Alkaline Magmatism in the Brazilian Platform (P. Comin-Chiaromonti &
- 393 C.B. Gomes, eds.) FAPESP, São Paulo (443–472).
- 394 BROTZU, P., MELLUSO, L., BENNIO, L., GOMES, C.B., LISTRINO, M., MORBIDELLI, L., MORRA, V.,
- 395 RUBERTI, E., TASSINARI, C.C.G., & D'ANTONIO, M. (2007) Petrogenesis of the Cenozoic potassic
- 396 alkaline complex of Morro de São João, southeastern Brazil. *Journal of South American Earth*
- 397 *Sciences*, **24**, 93–115.
- 398 CHAKRABARTY, A., MITCHELL, R.H., REN, M., PAL, S., PAL, S., & SEN, A.K. (2018) Nb–Zr–REE re-
- 399 mobilization and implications for transitional agpaitic rock formation: insights from the Sushina
- 400 Hill Complex, India. *Journal of Petrology*, **59**, 1899–1938.
- 401 CUCCINIELLO, C., TUCKER, R.D., JOURDAN, F., MELLUSO, L., & MORRA, V. (2016) The age and
- 402 petrogenesis of the alkaline magmatism of Ampasindava Peninsula and Nosy Be archipelago,
- 403 northern Madagascar. *Mineralogy and Petrology*, **110**, 309–331.
- 404 DE LA ROCHE, H., LETERRIER, P., GRANDCLAUDE, P., & MARCHAL, E. (1980) A classification of
- 405 volcanic and plutonic rocks using R1-R2 diagram and major element analyses. Its relationships
- 406 with current nomenclature. *Chemical Geology*, **29**, 183–210.
- 407 FERRONI, F.R., MELLO, C.L., & DESTRO, N. (2018) Tectonic control on the Cabo Frio anorogenic
- 408 magmatic lineament, Southeastern Brazil. *Journal of South American Earth Sciences*, **83**, 37–54.
- 409 ENRICH, G.E.R., RUBERTI, E., AZZONE, R.G., & GOMES, C.B. (2016) Eudialyte-group minerals from
- 410 the Monte de Trigo alkaline suite, Brazil: composition and petrological implications. *Brazilian*
- 411 *Journal of Geology*, **46**, 411–426.
- 412 GOMES, C.B., RUBERTI, E., COMIN-CHIARAMONTI, P., & AZZONE, R.G. (2011) Alkaline magmatism

- 413       in the Ponta Grossa Arch, SE Brazil: a review. *Journal of South American Earth Sciences*, **32**,  
414       152–168.
- 415       GOMES, C.B., ALVES, F.R., AZZONE, R.G., ENRICH, G.E.R., & RUBERTI, E. (2017) Geochemistry and  
416       petrology of the Búzios Island alkaline massif, SE, Brazil. *Brazilian Journal of Geology*, **47**(1),  
417       127–145.
- 418       GOMES, C.B., COMIN-CHIARAMONTI, P., AZZONE, R.G., RUBERTI, E., & ENRICH, G.E.R. (2018)  
419       Cretaceous carbonatites of the southeastern Brazilian Platform: a review. *Brazilian Journal of*  
420       *Geology*, **48**(2), 317–345.
- 421       GUALDA, G.A.R. & VLACH, S.R.F. (1996) Eudialita-eucolita do maciço alcalino de Poços de Caldas,  
422       MG-SP: químismo e correlação com o comportamento ótico. 39º Congresso Brasileiro de  
423       Geologia, Anais, **3**, 34–36.
- 424       GUARINO, V., AZZONE, R.G., BROTZU, P., GOMES, C.B., MELLUSO, L., MORBIDELLI, L., RUBERTI, E.,  
425       TASSINARI, C.C.G., & BRILLI, M. (2012) Magmatism and fenitization in the Cretaceous  
426       potassium-alkaline-carbonatitic complex of Ipanema São Paulo State, Brazil. *Mineralogy and*  
427       *Petrology*, **104**, 43–61.
- 428       GUARINO, V., WU, F.-Y., LUSTRINO, M., MELLUSO, L., BROTZU, P., GOMES, C.B., RUBERTI, E.,  
429       TASSINARI, C.C.G., & SVISERO, D.P. (2013) U-Pb ages, Sr-Nd- isotope geochemistry, and  
430       petrogenesis of kimberlites, kamafugites and phlogopite-picrites of the Alto Paranaíba Igneous  
431       Province, Brazil. *Chemical Geology*, **353**, 65–82.
- 432       GUARINO, V., WU, F.-Y., MELLUSO, L., GOMES, C.B., TASSINARI, C.C.G., RUBERTI, E., & BRILLI, M.  
433       (2017) U-Pb ages, geochemistry, C-O-Nd-Sr-Hf isotopes and petrogenesis of the Catalão II  
434       carbonatitic complex (Alto Paranaíba Igneous Province, Brazil): implications for regional-scale  
435       heterogeneities in the Brazilian carbonatite associations. *International Journal of Earth Sciences*  
436       (*Geol Rundsch*), **106**(6), 1963–1989.
- 437       GUPTA, A.K. (2015) Origin of potassium-rich silica-deficient igneous rocks. Springer, 536 p.,  
438       ISBN: 978-81-322-2082-1.

- 439 HAMILTON, D.L. (1961) Nephelines as crystallization temperature indicators. *Journal of Petrology*,  
440 **69**, 321–329.
- 441 HAMILTON, D.L. & MACKENZIE, W.S. (1965) Phase equilibrium studies in the system NaAlSiO<sub>4</sub>  
442 (nepheline) - KAlSiO<sub>4</sub> - (kalsilite) - SiO<sub>2</sub> - H<sub>2</sub>O. *Mineralogical Magazine*, **34**, 214–231.
- 443 HASUI, Y. & OLIVEIRA, M.A.F. (1984) Província Montiqueira, setor central. In O Pré-Cambriano do  
444 Brasil (F.F.M. Almeida & Y. Hasui, eds.), Editore Edgard Blucher, São Paulo, Brazil (308-334).
- 445 JOHNSEN, O. & GAULT, R.A. (1997) Chemical variation in eudialyte. *Neues Jahrbuch für  
446 Mineralogie-Abhandlungen*, **171**, 215–237.
- 447 JOHNSEN, O. & GRICE, J.D. (1999) The crystal chemistry of the eudialyte group. *The Canadian  
448 Mineralogist*, **37**, 865–891.
- 449 JOHNSEN, O., GRICE, J.D., & GAULT, R.A. (2001) The eudialyte group: a review. *Geology of  
450 Greenland Survey Bulletin*, **190**, 65–72.
- 451 LARSEN, A.O. (2010) The Langesundsfjord. History, Geology, Pegmatites, Minerals.  
452 Salzhermendorf, Germany: Bode, 239 pp.
- 453 LOCOCK, A.J. (2008) An Excel spreadsheet to recast analyses of garnet into end-member  
454 components, and a synopsis of the crystal chemistry of natural silicate garnets. *Computers &  
455 Geosciences*, **34**, 1769–1780.
- 456 LUSTRINO, M., DALLAI, L., GIORDANO, R., GOMES, C.B., MELLUSO, L., MORBIDELLI, L., RUBERTI,  
457 E., & TASSINARI, C.C.G. (2003) Geochemical and Sr-Nd-O Isotopic features of the Poços de  
458 Caldas alkaline massif (SP-MG, SE Brazil): relationships with the Serra do Mar analogues. *Short  
459 Papers – IV South American Symposium on Isotope Geology*, 593–595.
- 460 LUSTRINO, M., MELLUSO, L., BROTZU, P., GOMES, G.B., MORBIDELLI, L., MUZIO, R., RUBERTI, E., &  
461 TASSINARI, C.C.G. (2005) Petrogenesis of the early Cretaceous Valle Chico igneous complex  
462 (SE Uruguay): Relationships with Paraná-Etendeka magmatism. *Lithos*, **82**, 407–434.

- 463 LUSTRINO, M., CUCCINIELLO, C., MELLUSO, L., TASSINARI, C.C.G., DE' GENNARO, R., & SERRACINO,  
464 M. (2012) Petrogenesis of Cenozoic volcanic rocks in the NW sector of the Gharyan volcanic  
465 field, Libya. *Lithos*, **155**, 218–235.
- 466 MACDONALD, R., KARUP-MØLLER, S., & ROSE-HANSEN, J. (2007) Astrophyllite-group minerals  
467 from the Ilímaussaq complex, South Greenland. *Mineralogical Magazine*, **71**, 1–16.
- 468 MARKS, M.A.W. & MARKL, G. (2017) A global review of agpaitic rocks. *Earth-Science Reviews*  
469 **173**, 229–258.
- 470 MARKL, G., MARKS, M.A.W., & FROST, B.R. (2010) On the controls of oxygen fugacity in the  
471 generation and crystallization of peralkaline rocks. *Journal of Petrology*, **51**, 1831–1847.
- 472 MARKS, M.A.W., SCHILLING, J., COULSON, I.M., WENZEL, T., & MARKL, G. (2008) The Alkaline-  
473 Peralkaline Tamazeght Complex, High Atlas Mountains, Morocco: mineral chemistry and  
474 petrological constraints for derivation from a compositionally heterogeneous mantle source.  
475 *Journal of Petrology*, **49**(6), 1097–1131.
- 476 MARKS, M.A.W., HETTMANN, K., SCHILLING, J., FROST, B.R., & MARKL, G. (2011) The  
477 mineralogical diversity of alkaline igneous rocks: critical factors for the transition from miaskitic  
478 to agpaitic phase assemblages. *Journal of Petrology*, **52**, 439–455.
- 479 MACDONALD, R., KARUP-MØLLER, S., & ROSE-HANSEN, J. (2007) Astrophyllite-group minerals  
480 from the Ilímaussaq complex, South Greenland (contribution to the mineralogy of Ilímaussaq no.  
481 123). *Mineralogical Magazine*, **71**(1), 1–16.
- 482 MELLUSO, L., LUSTRINO, M., RUBERTI, E., BROTZU, P., GOMES, C.B., MORBIDELLI, L., MORRA, V.,  
483 SVISERO, D.P., & D'AMELIO, F. (2008) Major- and trace-element composition of olivine,  
484 perovskite, clinopyroxene, Cr-Fe-Ti oxides, phlogopites and host kamafugites and kimberlites,  
485 Alto Paranaíba, Brazil. *The Canadian Mineralogist*, **46**, 19–40.
- 486 MELLUSO, L., SRIVASTAVA, R.K., GUARINO, V., ZANETTI, A., & SINHA, A.K. (2010) Mineral  
487 compositions and magmatic evolution of the Sung Valley ultramafic-alkaline-carbonatitic

- 488 complex (NE India). *The Canadian Mineralogist*, **48**, 205–229,  
489 <https://dx.doi.org/10.3749/canmin.48.1.205>.
- 490 MELLUSO, L., DE' GENNARO, R., FEDELE, L., FRANCIOSI, L., & MORRA, V. (2012) Evidence of  
491 crystallization in residual, Cl–F-rich, agpaitic, trachyphonolitic magmas and primitive Mg-rich  
492 basalt–trachyphonolite interaction, in the lava domes of the Phleorean Fields (Italy). *Geological  
493 Magazine*, **149**, 532–550(551).
- 494 MELLUSO, L., MORRA, V., GUARINO, V., DE' GENNARO, R., FRANCIOSI, L., & GRIFA, C. (2014) The  
495 crystallization of shoshonitic to peralkaline trachyphonolitic magmas in a H<sub>2</sub>O-Cl-F- rich  
496 environment at Ischia (Italy), with implications for the feeder system of the Campania Plain  
497 volcanoes. *Lithos*, **201-211**, 242–259.
- 498 MELLUSO, L., GUARINO, V., LISTRINO, M., MORRA, V., & DE' GENNARO, R. (2017) The REE- and  
499 HFSE-bearing phases in the Itatiaia alkaline complex (Brazil), and geochemical evolution of  
500 feldspar-rich felsic melts. *Mineralogical Magazine*, **81**, 217–250.
- 501 MELLUSO, L., TUCKER, R.D., CUCCINIELLO, C., LE ROEX, A.P., MORRA, V., ZANETTI, A., &  
502 RAKOTOSON, R.L. (2018) The magmatic evolution and genesis of the Quaternary basanite-  
503 trachyphonolite suite of Itasy (Madagascar) as inferred by geochemistry, Sr-Nd-Pb isotopes and  
504 trace element distribution in coexisting phases. *Lithos*, **310-311**, 50–64.
- 505 MITCHELL, R. & LIFEROVICH, R. (2006) Subsolidus deuterian/hydrothermal alteration of eudialyte in  
506 lujavrite from the Pilansberg alkaline complex, South Africa. *Lithos*, **91(1-4)**, 352–372.
- 507 MONTES-LAUAR, C.R. (1988) Estudo Paleomagntico dos Maciço Alcalinos dos Poços de Caldas,  
508 Passa Quatro e Itatiaia. Unpublished MsD thesis, University of São Paulo, São Paulo, Brazil,  
509 101 p.
- 510 MORBIDELLI, L., GOMES, C.B., BECCALUVA, L., BROTZU, P., CONTE, A.M., RUBERTI, E., &  
511 TRAVERSA, G. (1995) Mineralogical, petrological and geochemical aspects of alkaline and  
512 alkaline-carbonatite associations from Brazil. *Earth-Science Reviews*, **39**, 135–168.

- 513 OLIVIO, G.R. & WILLIAMS-JONES, A.E. (1999) Hydrothermal REE-rich eudialyte from the  
514 Pilanesberg Complex, South Africa. *The Canadian Mineralogist*, **37**(3), 653–663.
- 515 PFAFF, K., WENZEL, T., SCHILLING, J., MARKS, M.A.W., & MARKL, G. (2010) A fast and easy-to-use  
516 approach to cation site assignment for eudialyte-group minerals. *Neues Jahrbuch Fur  
517 Mineralogie-Abhandlungen*, **187**, 69–81.
- 518 PIILONEN, P.C., LALONDE, A.E., McDONALD, A.M., & GAULT, R.A. (2003) Insights into  
519 astrophyllite-group minerals. I. Nomenclature, composition and development of a standardized  
520 general formula. *The Canadian Mineralogist*, **41**, 1–26.
- 521 POUCHOU, J.L. & PICHOIR, F. (1988) Microbeam Analysis. Newbury D. (ed.), San Francisco Press,  
522 315 p.
- 523 RIBEIRO, A.C., RICCOMINI, C., & LEITE, J.A.D. (2018) Origin of the largest South American  
524 transcontinental water divide. *Scientific Reports*, **8**, 17144.
- 525 RIBEIRO-FILHO, E. & CORDANI, U.G. (1966) Contemporaneidade das intrusões de rochas alcalinas  
526 do Itatiaia, Passa Quatro e Morro Redondo. Publ. nº, 1 do Núcleo do Rio de Janeiro, Sociedade  
527 Brasileira de Geologia, 62–63.
- 528 RICCOMINI, C., VELAZQUEZ, V.F., & GOMES, C.B. (2005) Tectonic controls of the Mesozoic and  
529 Cenozoic alkaline magmatism in the central-southeastern Brazilian Platform. In Mesozoic to  
530 Cenozoic Alkaline Magmatism in the Brazilian Platform (P. Comin-Chiaromonti & C.B. Gomes,  
531 eds.) FAPESP, São Paulo (31–55).
- 532 ROSA, P.A.S. & RUBERTI, E. (2018) Nepheline syenites to syenites and granitic rocks of the Itatiaia  
533 alkaline massif, southern Brazil: new geological and petrological insights into a migratory ring  
534 complex. *Brazilian Journal of Geology*, **48**, 347–372.
- 535 SCHMITT, A.K., EMMERMANN, R., TRUMBULL, R.B., & BÜHN, B. (2000) Petrogenetic aspects of  
536 metaluminous and per-alkaline granites in the Brandberg anorogenic complex, Namibia:  
537 Evidence for major mantle contribution. *Journal of Petrology*, **41**, 1207–1239.

- 538 SCHILLING, J., MARKS, M., WENZEL, T., & MARKL, G. (2009) Reconstruction of magmatic to  
539 subsolidus processes in an agpaitic system using eudialyte textures and composition: a case study  
540 from Tamazeght, Morocco. *The Canadian Mineralogist*, **47**(2), 351–365.
- 541 SCHILLING, J., WU, F.-Y., MCCAMMON, C., WENZEL, T., MARKS, M.A.W., PFAFF, K., JACOB, D.E.,  
542 & MARKL, G. (2011b) The compositional variability of eudialyte-group minerals. *Mineralogical  
543 Magazine*, **75**(1), 87–115.
- 544 SIGOLO, J.B. (1988) As formações bauxíticas do Maciço Alcalino de Passa Quatro, MG: sua  
545 Evolução micromorfológica, geoquímica e as implicações do relevo. Unpublished PhD thesis,  
546 University of São Paulo, São Paulo, Brazil, 186 pp.
- 547 SONOKI, L.K. & GARDA, G.M. (1988) Idades K-Ar de rochas alcalinas do Brasil Meridional e  
548 Paraguai Oriental: compilação e adaptação às novas constantes de decaimento. *Boletim IG-USP,  
549 Série Científica*, **19**, 63–85.
- 550 THOMPSON, R.N., GIBSON, S.A., MITCHELL, J.G., DICKIN, A.P., LEONARDOS, O.H., BROD, J.A., &  
551 GREENWOOD, J.C. (1998) Migrating Cretaceous-Eocene magmatism in the Serra do Mar  
552 alkaline Province, SE Brazil: melts from the deflected Trindade mantle plume? *Journal of  
553 Petrology*, **39**, 1493–1526.
- 554 ULRICH, H.H.G.J., VLACH, S.R.F., ULRICH, M.N.C., & KAWASHITA, K. (2002)  
555 Penecontemporaneous syenitic-phonolitic and basic-ultrabasic-carbonatitic rocks at the Poços  
556 de Caldas alkaline massif, SE Brazil: geological and geochronological evidence. *Revista  
557 Brasileira de Geociências*, **32**, 15–26.
- 558 VLACH, S.R.F., ULRICH, H.H.G.J., ULRICH, M.N.C., & VASCONCELOS, P.M. (2018) Melanite-  
559 bearing nepheline syenite fragments and  $^{40}\text{Ar}/^{39}\text{Ar}$  age of phlogopite megacrysts in conduit  
560 breccia from the Poços de Caldas Alkaline Massif (MG/SP), and implications. *Brazilian Journal  
561 of Geology*, **48**(2), 391–402.
- 562 WOOLLEY, A.R. & PLATT, R.G. (1988) The peralkaline nepheline syenites of the Junguni intrusion,  
563 Chilwa province, Malawi. *Mineralogical Magazine*, **52**, 425–433.

564 WU, B., WANGA, R.-C., YANG, J.-H., WU, F.-Y., ZHANG, W.-L., GU, X.-P., & ZHANG, A.-C. (2016)  
565      Zr and REE mineralization in sodic lujavrite from the Saima alkaline complex, northeastern  
566      China: A mineralogical study and comparison with potassic rocks. *Lithos*, **262**, 232–246.  
567 WU, F.-Y., YANG, Y.-H., MARKS, M.A.W., LIU, Z.-C., ZHOU, Q., GE, W.-C., YANG, J.-S., ZHAO, Z.-  
568      S., MITCHELL, R.H., & MARKL, G. (2010) In situ U-Pb, Nd and Hf isotopic analysis of eudialyte  
569      by LA-(MC)-ICP-MS. *Chemical Geology*, **273(1-2)**, 8–34.  
570  
571      Figure captions:  
572      FIG. 1: (a) Alkaline provinces of southeastern Brazil and their relationships with major structural  
573      features (modified after Melluso *et al.* 2017): 1) Late Ordovician to Early Cretaceous Paraná  
574      Basin; 2) Early Cretaceous tholeiitic lava flows; 3) Late Cretaceous Bauru Basin; 4) Offshore  
575      marginal basins; 5) Alkaline provinces; 6) Age of alkaline rocks (diamonds: Permian-Triassic;  
576      squares: Early Cretaceous; triangles: Late Cretaceous; circles: Paleogene); 7) Axes of main arcs  
577      (AX, Alto Xingu; SV, São Vicente; BJ, Bom Jardim de Goiás; PG, Ponta Grossa; RG, Rio  
578      Grande; PP, Ponta Porã); 8) Torres Syncline; 9) Major fracture zones, in part deep lithospheric  
579      faults (Rifts: MR, Mercedes; RM, Rio das Mortes; MG, Moirão; SR, Santa Rosa; AR, Asunción;  
580      Lineaments: TB, Transbrasiliiano; AP, Alto Paranaíba; MJ, Moji-Guaçu; CF, Cabo Frio; RT, Rio  
581      Tietê; SL, São Carlos-Leme; PR, Paranapanema; PI, Piedade; GP, Guapiara; JC, São Jerônimo-  
582      Curiúva; RA, Rio Alonzo; PQ, Rio Piquiri; AM, Santa Lucia-Aiguá-Merin). Insets: 1) Paraná  
583      Basin contour. (b) Sketch map of the Passa Quatro intrusion (modified after Brotzu *et al.* 1992)  
584      with location of the studied samples. (c) R1-R2 classification diagram (De La Roche *et al.* 1980).  
585      (d) Differentiation Index (D.I.) vs. Peralkaline Index (P.I) diagram for the Passa Quatro rocks.  
586      The data of syenites and phonolites of Morro Redondo, Itatiaia, Poços de Caldas, Morro de São  
587      João and Montiquiera Range are taken from Brotzu *et al.* (1989, 1992, 2007), Lustrino *et al.*  
588      (2003), Azzone *et al.* (2018) and Melluso *et al.* (2017).  
589      FIG. 2. Petrographic characteristics of main Passa Quatro nepheline syenites and PQ42 phonolite.

590 Abbreviations: ae, aegirine; afs, alkali feldspar; ast, astrophyllite; bt, biotite; cpx, clinopyroxene;  
591 F-dis, F-disilicate; ne, nepheline; op, opaque minerals; ttn, titanite.

592 FIG. 3. Back-scattered images of main accessory minerals in Passa Quattro nepheline syenites and  
593 PQ42 phonolite. Abbreviations: alk, alkali feldspar; anl, analcime; ap, apatite; cpx,  
594 clinopyroxene; fluo, fluorite; hiort, hiortdahlite; låv, lavenite; mgt, magnetite; ros, rosenbuschite;  
595 wöh, wöhlerite; ttn, titanite; zirc, zircon.

596 FIG. 4. Nepheline-kalsilite-silica diagram (wt.%) for the rocks of Passa Quattro. Univariant lines  
597 from Hamilton & Mackenzie (1965) and Gupta (2015). The composition of the nephelines is also  
598 reported. The Morozevicz and Buerger compositions are the black dots.

599 FIG. 5. (a) Representative ternary plot of Passa Quattro eudialytes compared with those of Monte de  
600 Trigo (Enrich *et al.* 2016), Sushina Hill (Chakrabarty *et al.* 2018), Gharyan (Lustrino *et al.* 2012)  
601 and Ampasindava (Cucciniello *et al.* 2016). The diagram shows also the trend lines of the main  
602 eudialytes in other complexes (Gualda & Vlach 1996; Johnsen & Gault 1997; Olivio &  
603 Williams-Jones 1999; Johnsen & Grice 1999; Mitchell & Liferovich 2006; Marks *et al.* 2008;  
604 Schilling *et al.* 2009, 2011; Wu *et al.* 2010), modified after Enrich *et al.* (2016). (b) Binary  
605 diagram of Passa Quattro astrophyllite-group minerals. Astrophyllite from Ilímaussaq  
606 (Macdonald *et al.* 2007) and kupletskite from Sushina Hill (Chakrabarty *et al.* 2018) are plotted  
607 to comparison. (c) Apatite-britholite composition of Passa Quattro rocks, compared with Itatiaia  
608 trend (Melluso *et al.* 2017).

609 FIG. 6. (a), (b) and (c). Chemical composition of the F-disilicates in the Passa Quattro nepheline  
610 syenites. The reference compositions (black diamond) are those in the handbook of mineralogy  
611 of the MSA (names underlined). Reference compositions are from Phleorean Fields (Melluso *et*  
612 *al.* 2012), Ischia (Melluso *et al.* 2014), Gharyan (Lustrino *et al.* 2012), Itatiaia (Melluso *et al.*  
613 2017) and Sushina Hill (Chakrabarty *et al.* 2018). The reference compositions of the Oslo Rift  
614 nepheline syenites are taken from Andersen *et al.* (2010, 2012a,b). The structural formulae have  
615 been calculated assuming Si+Al=8 cations.

616 FIG. 7. Crystallization scheme on the evolution of Passa Quatro rocks.

617 FIG. 8. REE diagrams of the main complexes in the Serra do Mar Province.

618

619 Table caption:

620 TABLE 1. The crystal chemical formulas of minerals analyzed in the Passa Quatro rocks. Note: The  
621 symbol □ is the vacancy in the site.

622 TABLE 2. Representative compositions of typical accessory minerals analyzed in the Passa Quatro  
623 rocks.

624 TABLE 3. Representative compositions of F-disilicates. Cations are listed following site occupancy,  
625 according to their formula.

626

627 Supplementary Tables:

628 Supplementary Table A1. Minerals analyzed in the main Passa Quatro rocks.

629 Supplementary Table A2. Titanite

630 Supplementary Table A3. Eudialyte

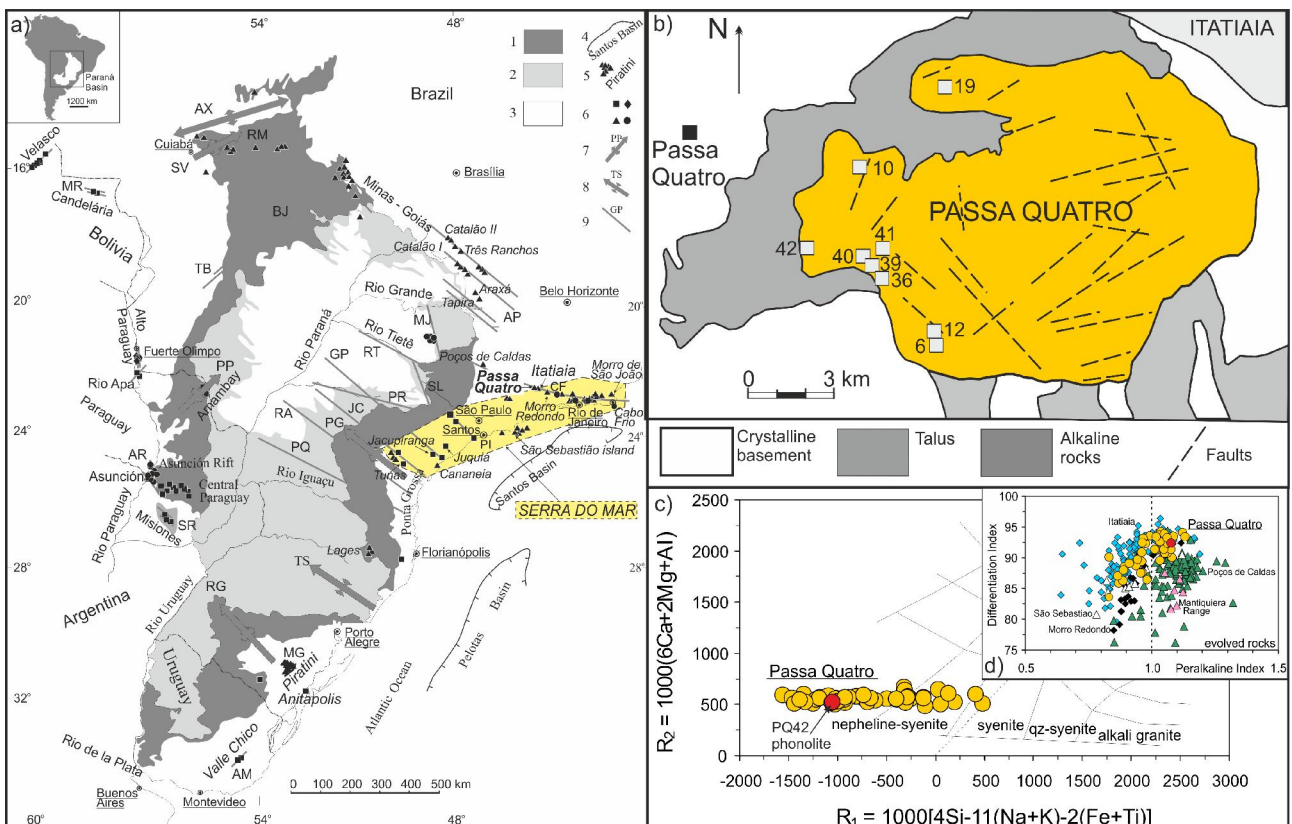
631 Supplementary Table A4. Astrophyllite and Kupletskite

632 Supplementary Table A5. F-Disilicates

633 Supplementary Table A6. Phosphates and Silicophosphates

634 Supplementary Table A7. Other accessory phases

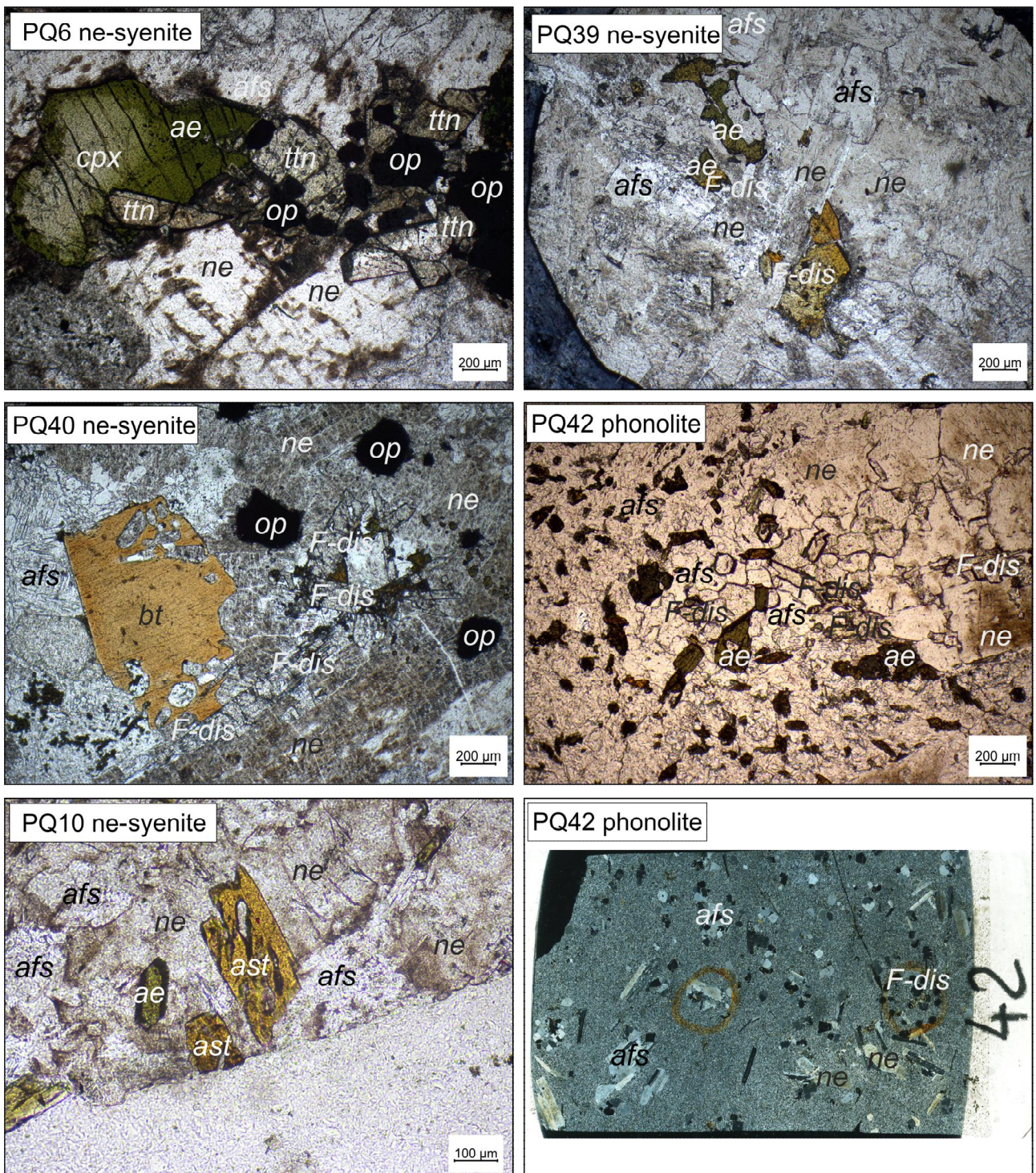
635



636

637 Figure 1

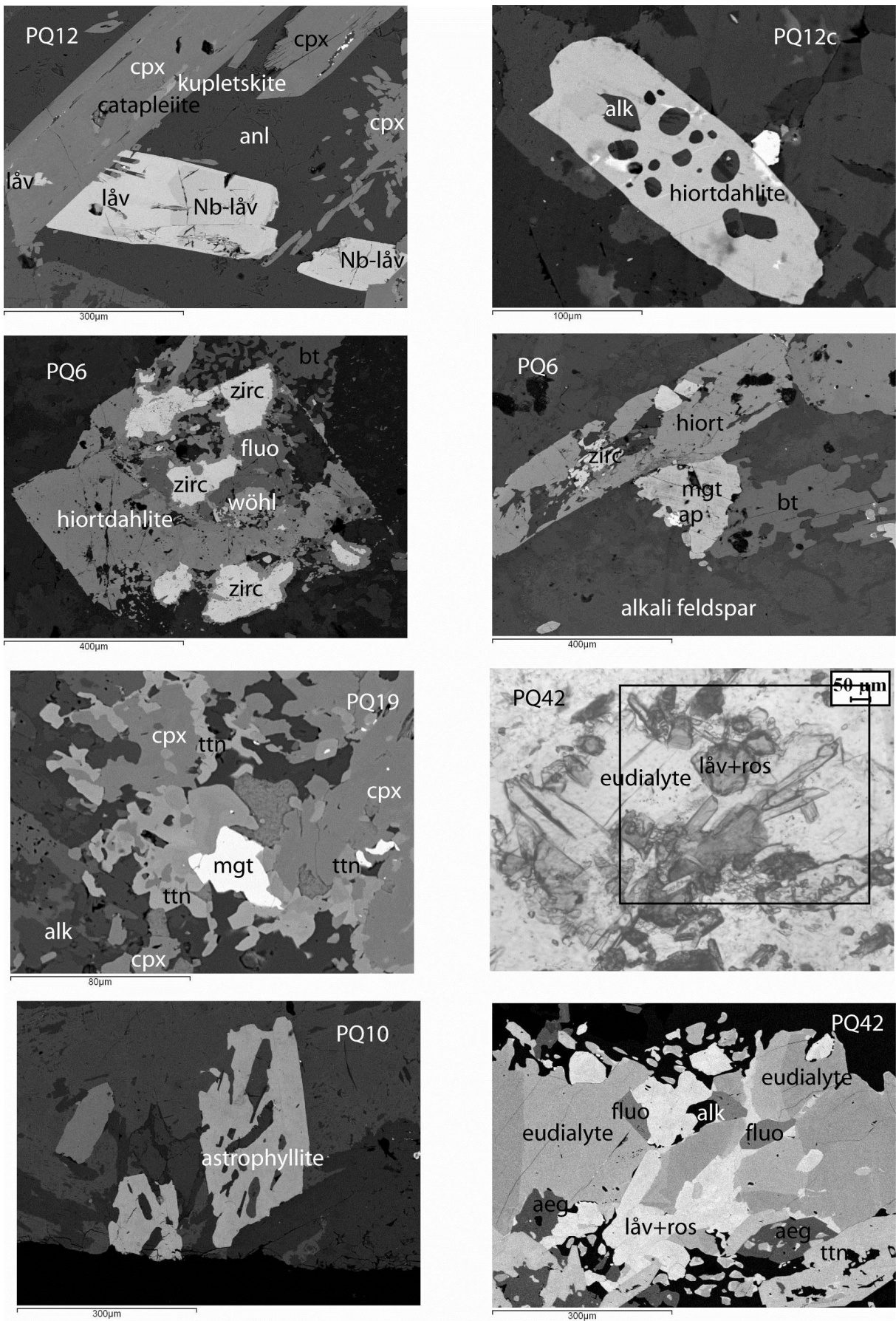
638

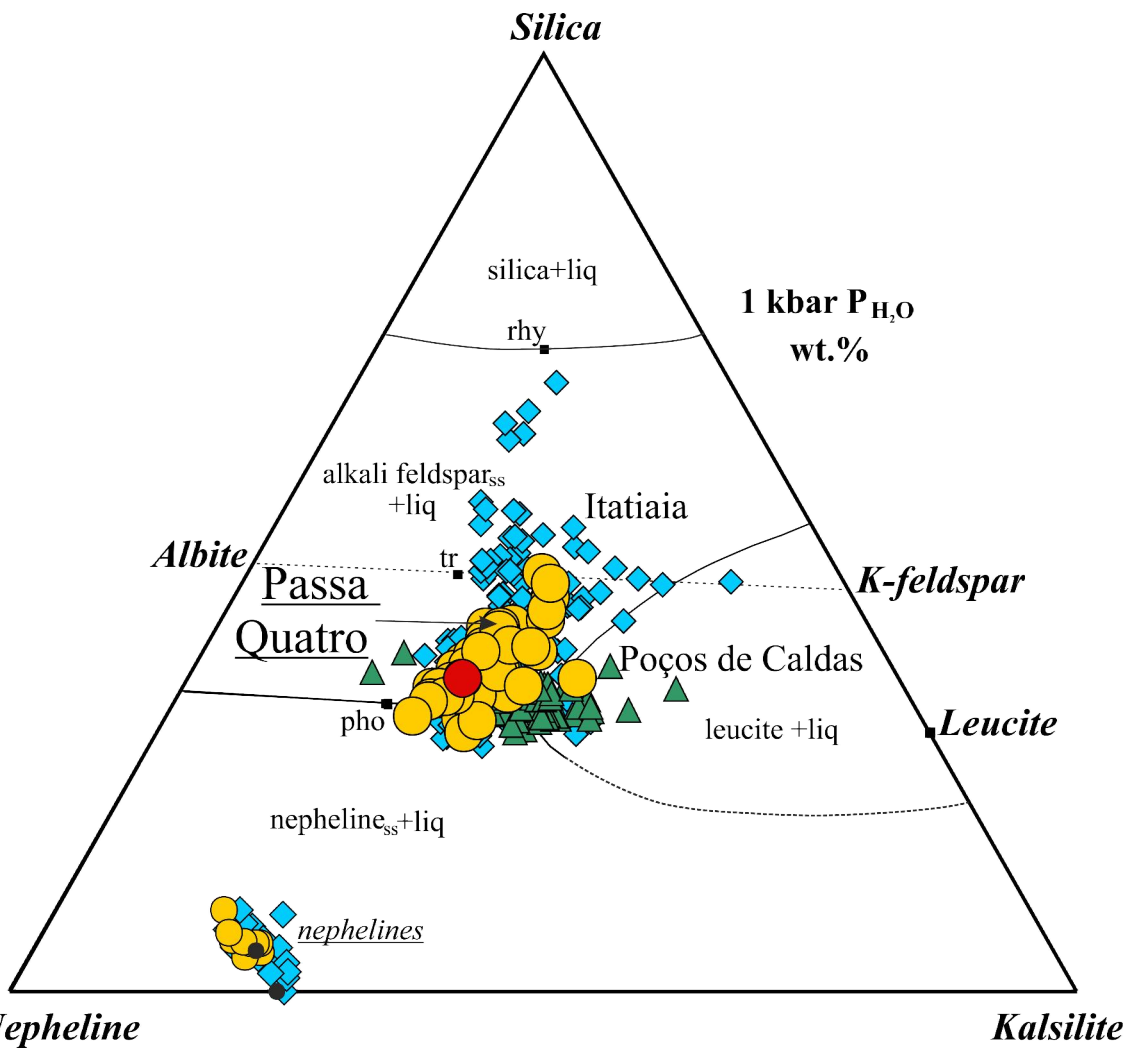


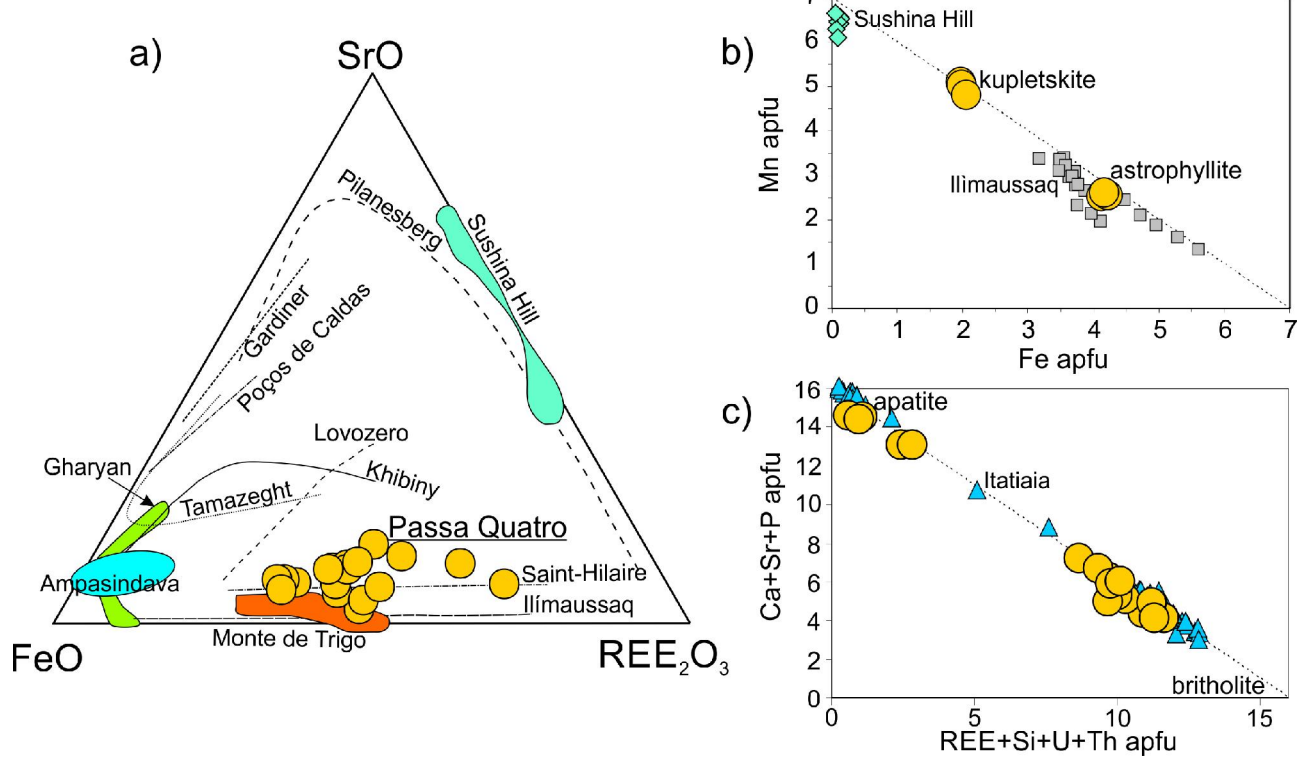
639

640 Figure 2

641



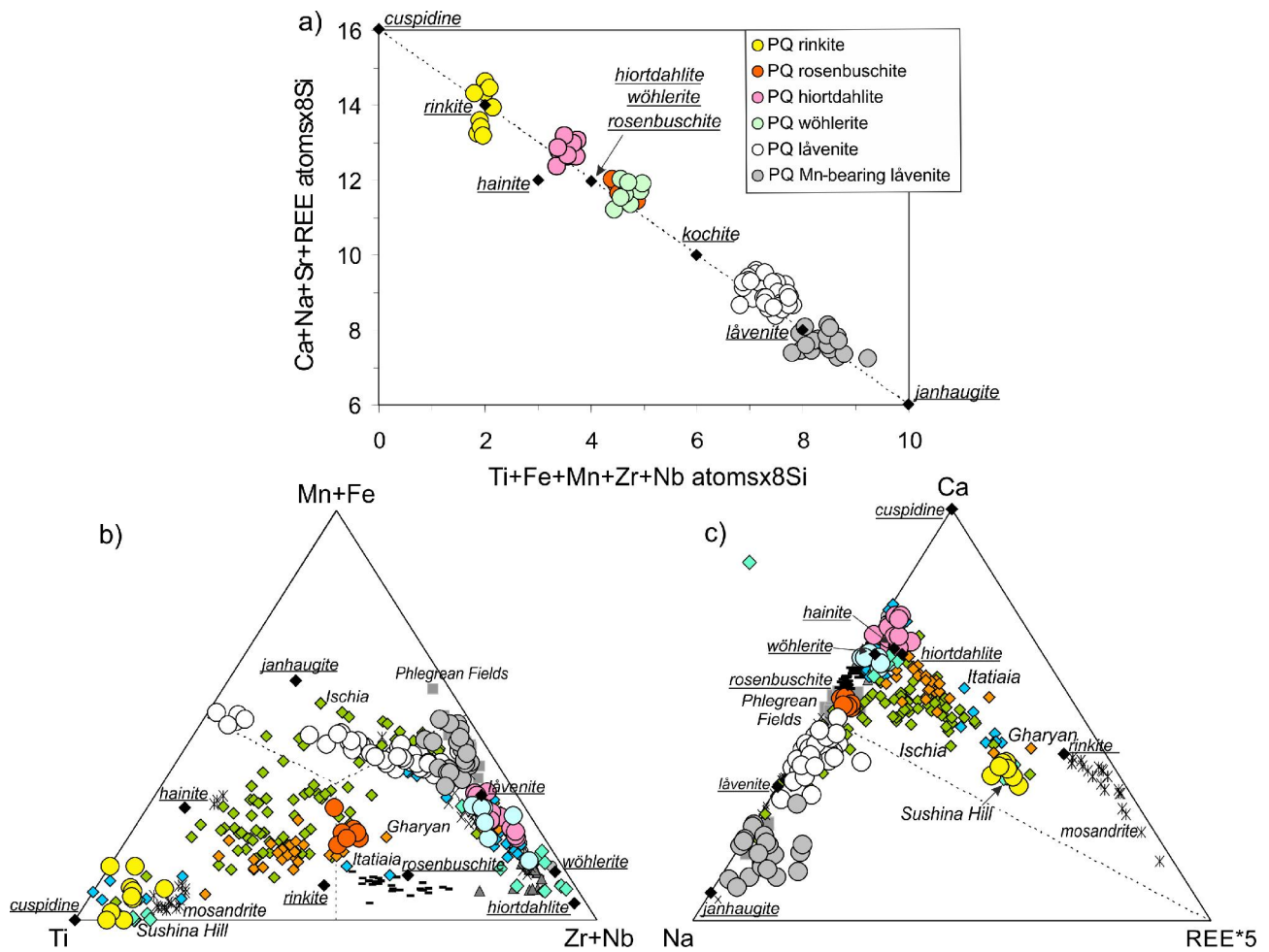




647

648 Figure 5.

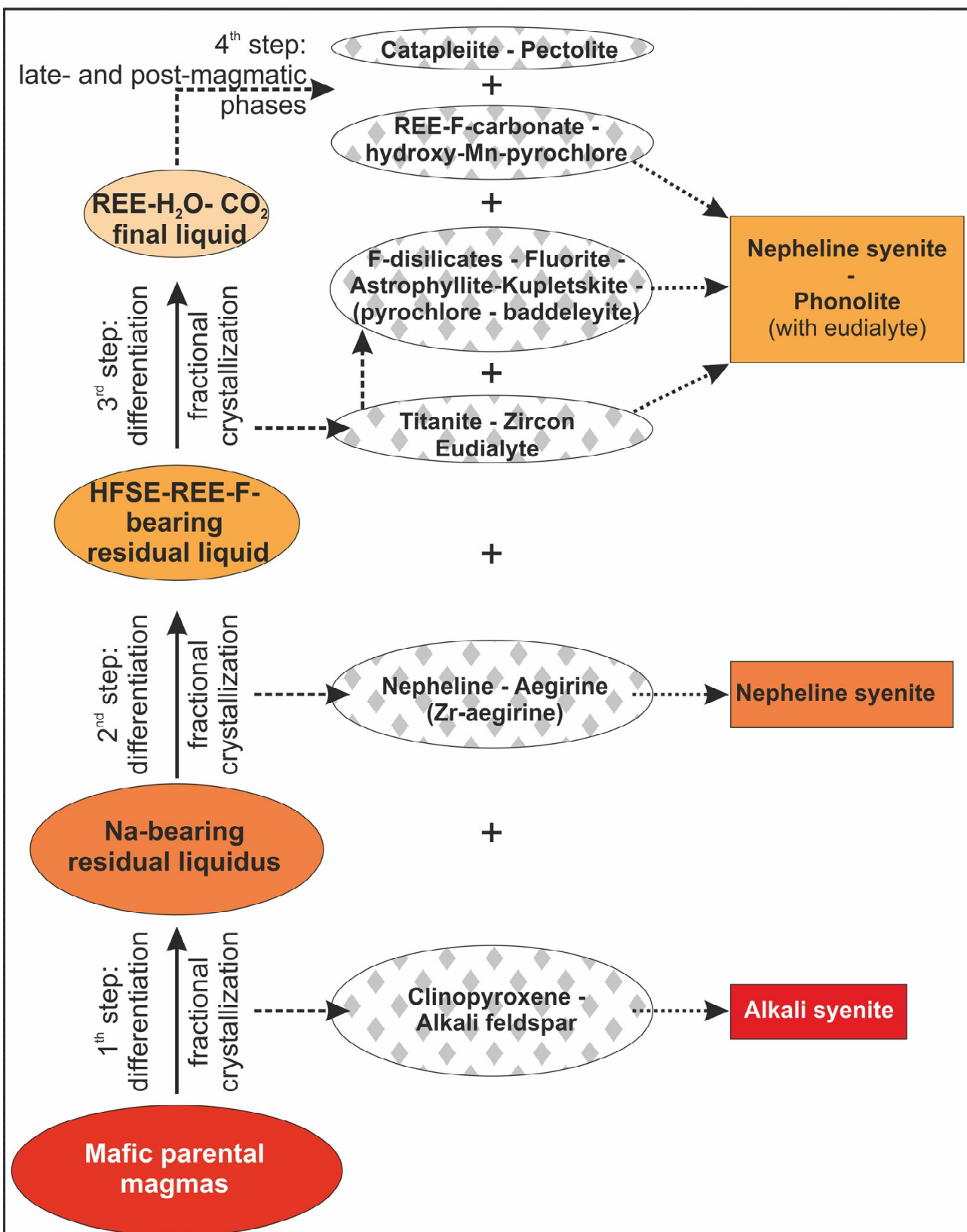
649



650

651 Figure 6

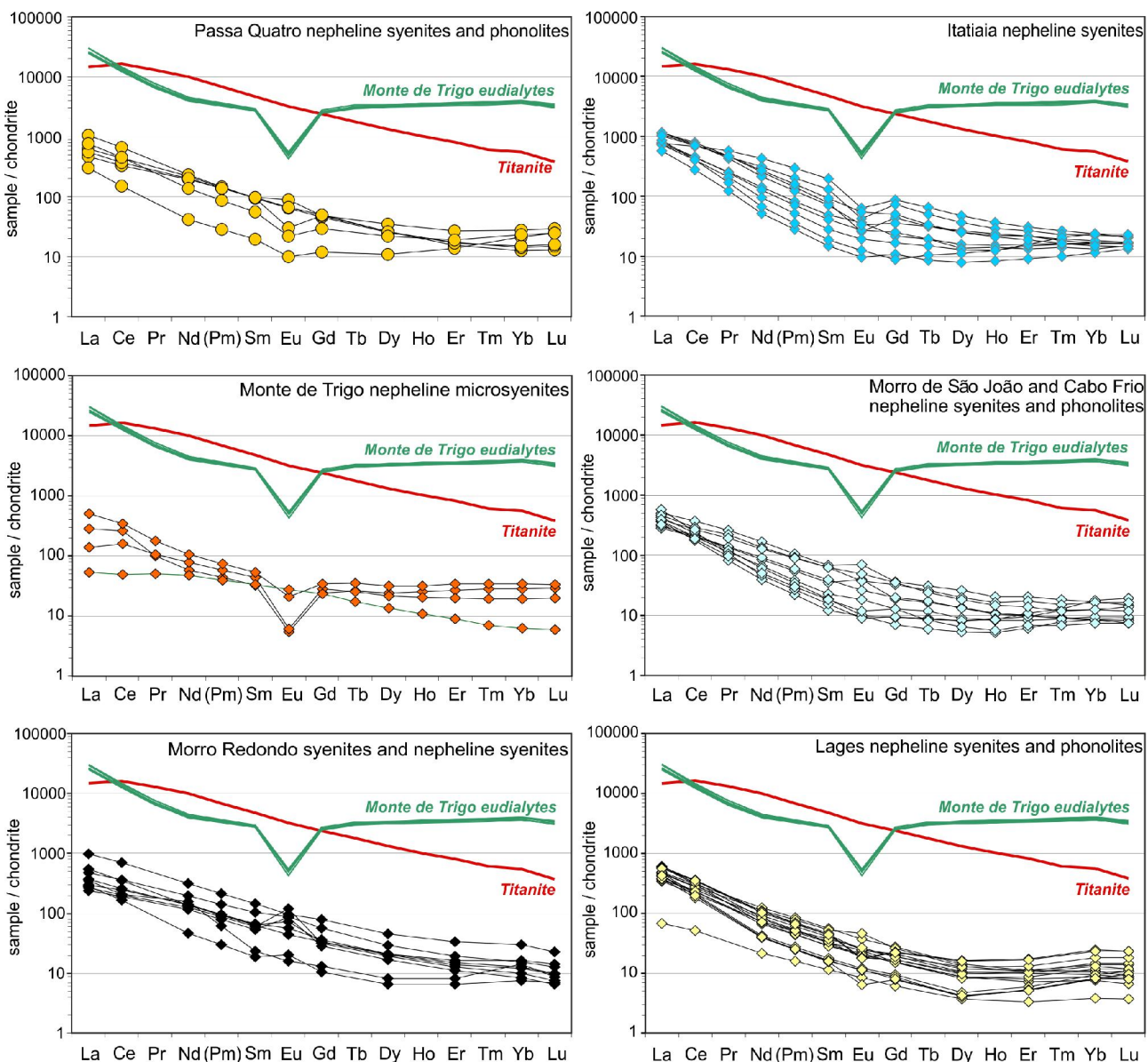
652



653

654 Figure 7

655



656

657 Figure 8

658

659 TABLE 1. THE CRYSTAL CHEMICAL FORMULAS OF MINERALS ANALYZED IN THE PASSA QUATRO  
 660 ROCKS. NOTE: THE SYMBOL  $\square$  IS THE VACANCY IN THE SITE.  
 661

662 Alkali-feldspar  $[(K_{2.14-3.96}, Na_{0-1.77}, Ca_{0-0.13}, Sr_{0-0.09}, Ba_{0-0.03})_{\Sigma=4-4.15} (Al_{3.63-3.88}, Fe_{0-0.09}, Na_{0.05-0.33})_{\Sigma=4} (Si_{11.72-11.91},$   
 663  $Al_{0.09-0.28})_{\Sigma=12}] O_{32}$

664 Plagioclase  $[(Na_{3.73-3.92}, Ca_{0-0.26}, K_{0-0.07}, Sr_{0-0.09}, Ba_{0-0.02})_{\Sigma=3.96-4} (Al_{3.41-4}, Fe_{0-0.13}, Na_{0-0.46})_{\Sigma=4} (Si_{10.01-11.99},$   
 665  $Al_{0.01-1.99})_{\Sigma=12}] O_{32}$

666 Nepheline  $[(Na_{5.91-6.22}, K_{1.11-1.52}, Ca_{0-0.06}, Sr_{0.04-0.11})_{\Sigma=7.26-7.75} (Al_{7.03-7.50}, Fe_{0.07-0.18}, Si_{0.40-0.84})_{\Sigma=7.91-8.06} Si_8 O_{32}]$

667 Clinopyroxene/ Aegirine  $[(Ca_{0.05-0.89}, Na_{0.12-0.91})_{\Sigma=0.95-1.03} (Mg_{0.01-0.48}, Mn_{0.04-0.16}, Fe_{0.43-0.87}, Ti_{0.02-0.08}, Cr_{0-0.06}, Zr_{0-0.01})_{\Sigma=0.94-1.08} (Si_{1.90-1.99}, Al_{0-0.08})_{\Sigma=1.96-2.03}] O_6$

669 Amphibole  $[(Na_{1.17-3.03}, Ca_{0.12-1.65}, K_{0.29-0.37}, Sr_{0.02-0.07})_{\Sigma=3.13-3.59} (Fe^{2+}_{1.57-3.05}, Fe^{3+}_{0.11-0.90}, Mg_{0.72-1.92}, Mn_{0.40-0.69}, Ti_{0.13-0.35}, ^VI Al_{0-0.14})_{\Sigma=5-5.08} (Si_{6.14-7.84}, ^IV Al_{0.16-1.88})_{\Sigma=7.92-8} O_{22} (OH_{0.63-2}, F_{0-1.37})_{\Sigma=2}]$

671 Titanite  $[(Ca_{0.91-1.04}, Na_{0-0.07}, Sr_{0-0.02}, LREE_{0-0.08})_{\Sigma=0.99-1.09} (Ti_{0.69-0.92}, Al_{0-0.08}, Fe^{2+}_{0.03-0.11}, Mn_{0-0.01}, Zr_{0-0.06}, Nb_{0-0.13})_{\Sigma=0.91-1.04} Si_{0.98-1.12} O_5]$

674 Eudialyte-group minerals

675 Eudialyte  $[(Na_{10.87-13.45}, K_{0-0.31}, Mn_{0.32-1.70}, Sr_{0.07-0.37}, La_{0.11-0.69}, Ce_{0.13-0.64}, Nd_{0-0.21}, \square_{0.24-2.96})_{\Sigma=15-15.26} (Ca_{5-5.85}, Mn_{0.15-1})_{\Sigma=6} (Fe_{1.33-2.27}, Mn_{0.73-1.67})_{\Sigma=3} (Zr_{2.65-3}, Ti_{0.02-0.17}, Nb_{0-0.18})_{\Sigma=3} (Si_{0.89-1.68}, Nb_{0.08-0.80}, Ti_{0-0.35}, Al_{0-0.21}, Zr_{0-0.22})_{\Sigma=2} (Si_{24}O_{72}) (O, OH, H_2O)_3 (Cl, OH)_{\Sigma=2}]$

678 Kentbrooksite  $[(Na_{12.26}, K_{0.24}, Sr_{0.96}, La_{0.73}, Ce_{0.80})_{\Sigma=14.99} (Ca_{5.05}, Fe_{0.95})_{\Sigma=6} Mn_{3.01} Zr_{2.99} (Nb_{0.54}, Ti_{0.06}, Al_{0.05}, Mg_{0.04}, Fe_{0.28}, Pb_{0.05}, U_{0.05})_{\Sigma=1.07} (Si_{24.80} O_{74}) F_{1.81} \cdot 2H_2O]$

681 F-disilicates

682 Rinkite  $[(Ca_{5.49-6.60}, Ce_{0.94-1.19}, La_{0.37-0.65}, Nd_{0.07-0.29}, Sm_{0-0.04})_{\Sigma=7.01-8.50} Na_2 (Na_{2.27-2.77}, Ca_{1.23-1.73})_{\Sigma=4} (Ti_{1.63-1.81}, Fe_{0-0.14}, Mn_{0-0.13}, Mg_{0-0.08}, Zr_{0-0.05}, Nb_{0.05-0.19})_{\Sigma=1.80-2.09} (Si_{7.91-8}, Al_{0-0.09})_{\Sigma=8} O_{28} F_4 (O_{1.87-3.57}, F_{4.43-6.13})_{\Sigma=4}]$

685 Rosenbuschite  $[(Ca_{6.24-6.54}, Na_{5.22-5.38}, Sr_{0.06-0.09}, La_{0-0.04}, Ce_{0-0.04}, Nd_{0-0.04}, Sm_{0-0.03})_{\Sigma=11.65-12.03} (Zr_{1.50-1.84}, Ti_{1.54-1.83}, Fe_{0.07-0.26}, Mn_{0.76-0.98}, Mg_{0-0.05}, Nb_{0.07-0.18})_{\Sigma=4.40-4.71} (Si_{7.91-7.99}, Al_{0.01-0.09})_{\Sigma=8} O_{28} (O_{2.08-3.05}, F_{4.95-5.92})_{\Sigma=8}]$

688 Hiortdahlite  $[(Ca_{7.92-9.46}, Na_{3.03-3.80}, Sr_{0.02-0.17}, Y_{0-0.12}, La_{0-0.06}, Ce_{0-0.11}, Nd_{0-0.06}, Sm_{0-0.05})_{\Sigma=11.73-12.82} (Zr_{1.83-2.38}, Ti_{0.16-0.31}, Fe_{0.15-0.35}, Mn_{0.50-0.85}, Mg_{0-0.08}, Nb_{0.20-0.38}, Ca_{0.25-0.64})_{\Sigma=4} (Si_{7.96-8}, Al_{0-0.04})_{\Sigma=8} O_{28} (O_{2.41-2.98}, F_{5.02-5.59})_{\Sigma=8}]$

691 Wöhlerite  $\{(Na_{3.77-4.09}, Ca_{0-0.71}, Sr_{0.08-0.15}, Y_{0-0.12}, La_{0-0.05}, Ce_{0-0.10}, Nd_{0-0.03}, Sm_{0-0.09})_{\Sigma=4.06-4.87} (Ca_{7.03-7.55}, Fe_{0.12-0.25}, Mg_{0.06-0.26}, Mn_{0.09-0.57})_{\Sigma=7.61-8.11} (Zr_{1.71-1.88}, Nb_{1.07-1.87}, Ti_{0.16-0.48}, Mn_{0.17-0.72})_{\Sigma=4} (Si_{7.84-8}, Al_{0-0.16})_{\Sigma=8} O_{28} [(O, OH)_{4.18-5.87} F_{2.13-3.82}]_{\Sigma=8}\}$

694 Låvenite  $\{[(Na_{4.46-5.95}, Ca_{1.92-3.43}, Sr_{0-0.19}, Y_{0-0.03}, La_{0-0.15}, Ce_{0-0.11}, Nd_{0-0.06}, Sm_{0-0.07})_{\Sigma=8} (Mn^{2+}_{1.62-2.59}, Fe^{2+}_{0.61-1.40}, Ti_{0-0.83}, Mg_{0-0.19}, Ca_{0.39-1.61})_{\Sigma=3.80-4.37} (Zr_{0.03-3.20}, Ti_{0.22-3.63}, Nb_{0.10-0.95})_{\Sigma=3.66-4} (Si_{7.90-8}, Al_{0-0.10})_{\Sigma=8} O_{28} [(O, OH)_{2.77-5.37} F_{2.63-5.23}]_{\Sigma=8}\}$

697 Mn-bearing låvenite  $\{[(Na_{5.50-6.98}, Ca_{0.66-2.39}, Sr_{0-0.22}, La_{0-0.12}, Ce_{0-0.10}, Nd_{0-0.06}, Sm_{0-0.08}, Nb_{0-1.11})_{\Sigma=7.38-8.60} (Mn^{2+}_{2.27-3.68}, Fe^{2+}_{0.38-0.76}, Ti_{0-0.58}, Mg_{0-0.11}, Nb_{0.08-0.68})_{\Sigma=3.80-4.37} (Zr_{2.98-4.41}, Ti_{0.01-0.98}, Nb_{0-0.63})_{\Sigma=4-4.41} (Si_{7.92-8}, Al_{0-0.08})_{\Sigma=8} O_{28} [(O, OH)_{3.01-6.50} F_{1.50-4.99}]_{\Sigma=8}\}$

701 TABLE 1. CONTINUED.

703 *Astrophyllite-group minerals*

704	<u>Astrophyllite</u>	$\{(K_{1.74-1.84}, Na_{1.22-1.33}, Ca_{0.38-0.43}, Sr_{0.04-0.08})_{\Sigma=3.41-3.61} (Fe^{2+}_{4.12-4.21}, Mn_{2.53-2.61}, Mg_{0.31-0.35})_{\Sigma=6.99-7.12}$ $(Ti_{1.50-1.68}, Nb_{0.08-0.16}, Al_{0.31-0.50}, Zr_{0.19-0.41})_{\Sigma=2.35-2.45} (Si_{7.67-7.85}, Al_{0.15-0.33})_{\Sigma=8} O_{24} [F_{1.55-1.94}, (O, OH)_{5.06-5.45}]_{\Sigma=7}\}$
707	<u>Kupletskite</u>	$\{(K_{1.65-1.78}, Na_{1.14-1.18}, Ca_{0.35-0.39}, Sr_{0.13-0.21})_{\Sigma=3.27-3.52} (Mn_{4.82-5.11}, Fe^{2+}_{1.97-2.05}, Mg_{0.12-0.14})_{\Sigma=6.99-7.21}$ $(Ti_{1.39-1.51}, Nb_{0-0.01}, Al_{0.21-0.42}, Zr_{0.45-0.57})_{\Sigma=2.16-2.51} (Si_{7.79-7.80}, Al_{0.20-0.21})_{\Sigma=8} O_{24} [F_{1.38-2.02} (O, OH)_{5.98-5.62}]_{\Sigma=7}\}$

711 *Phosphates and Silicophosphates*

712	<u>Apatite</u>	$[(Ca_{8.27-9.14}, Na_{0.04-0.14}, Fe_{0-0.09}, Sr_{0.01-0.56}, La_{0.17-0.44}, Ce_{0.18-0.81}, Nd_{0.01-0.18}, Sm_{0-0.05}, Th_{0-0.03}, U_{0-0.01})_{\Sigma=9.52-9.98} (P_{4.70-5.61}, Si_{0.18-1.35}, S_{0-0.03})_{\Sigma=5.80-6.08} O_{12} (F_{0.76-1.95}, Cl_{0-0.03}, OH_{0.04-1.24})_{\Sigma=2}]$
714	<u>Britholite</u>	$[(Ce_{2.46-3.13}, La_{1.43-2.93}, Nd_{0.14-0.96}, Sm_{0-0.06}, Ca_{2.89-5.43}, Na_{0-0.73}, Fe_{0-0.04}, Sr_{0.01-0.57}, Y_{0-0.41}, Th_{0.05-0.12}, U_{0-0.05})_{\Sigma=9.73-10.18} (Si_{4.06-5.73}, P_{0.17-1.73}, S_{0-0.05})_{\Sigma=5.71-6.19} O_{12} (F_{0.31-1.63}, Cl_{0-0.05}, OH_{0.35-1.69})_{\Sigma=2}]$

717 *Other minor accessory phases*

718	<u>Zircon</u>	$[(Zr_{0.95-1.01}, Hf_{0-0.04}, Y_{0-0.03}, La_{0-0.01}, Ce_{0-0.01}, Sm_{0-0.01}, Th_{0-0.01}, U_{0-0.01})_{\Sigma=2-2.01} Si_{0.99-1} O_4)]$
719	<u>Garnet</u>	$\{[(Ca_{2.82-2.87}, Fe^{2+}_{0-0.04}, Mn^{2+}_{0.07-0.13}, Mg_{0-0.05})_{\Sigma=2.96-3} (Fe^{3+}_{1.58-1.85}, Ti_{0.01-0.10}, Al_{0.07-0.40}, Fe^{2+}_{0-0.02}, Mn^{3+}_{0-0.09}, Mg_{0-0.06})_{\Sigma=2-2.04} (Si_{2.89-2.99}, Al_{0.01-0.11})_{\Sigma=3} (O_4)_3]\}$
721	<u>Pyrochlore</u>	$[(Ca_{0.75-1.12}, Na_{0.45-0.98}, Mn_{0-0.03}, Sr_{0-0.03}, La_{0.01-0.05}, Ce_{0.01-0.10}, Pr_{0-0.01}, Nd_{0-0.01}, Sm_{0-0.01}, Dy_{0-0.03}, Er_{0-0.02}, Yb_{0-0.02}, Th_{0-0.01}, U_{0.01-0.12}, \square_{0.01-0.43})_{\Sigma=2} (Nb_{1.29-1.81}, Ta_{0-0.07}, Ti_{0.14-0.56}, Fe_{0-0.05}, Si_{0.09-0.22})_{\Sigma=2} O_6 (OH_{0-0.26}, F_{0.74-1.21})]$
724	<u>Hydroxymanganopyrochlore</u>	$[(Mn_{1.36-2.01}, Ca_{0-0.24}, Na_{0.08-0.30}, Sr_{0-0.02}, Y_{0-0.01}, Ce_{0.01}, Gd_{0-0.01}, Er_{0-0.01}, \square_{0-0.04})_{\Sigma=2-2.13} (Ti_{1.27-1.64}, Nb_{0.26-0.630}, Ta_{0-0.01}, Fe_{0.09-0.10})_{\Sigma=2} O_6 (OH_{0.69-0.84}, F_{0.03-0.09}, Cl_{0.13-0.22})]$
726	<u>Catapleiite</u>	$[(Na_{1.33-1.59}, Ca_{0.02-0.12}, Mn_{0-0.02}, Fe_{0.03-0.06}, Sr_{0.04-0.09}, La_{0-0.01}, Ce_{0-0.01}, Nd_{0-0.02}, Sm_{0-0.01}, Nb_{0.01-0.06}, \square_{0.23-0.45})_{\Sigma=2} Zr_{0.99-1.04} Si_{2.97-3.02} O_9 \cdot 2(H_2O, F_{0.08-0.35}, Cl_{0-0.01})]$
728	<u>Pectolite</u>	$[Na_1 (Ca_{1.37}, Mn_{0.67}, Fe_{0.01}, Mg_{0.01})_{\Sigma=2.06} Si_{2.96} O_8 (OH_{0.87}, F_{0.12}, Cl_{0.01})_{\Sigma=1}]$

730

TABLE 2. Representative compositions of typical accessory minerals analyzed in the Passa Quatro rocks.

	<i>Titanite</i> PQ19	<i>Titanite</i> PQ41	<i>Eudialyte</i> PQ42	<i>Eudialyte</i> PQ42	<i>Kentsbrookite</i> PQ39	<i>Astrophyllite</i> PQ10	<i>Kupletsksite</i> PQ12	<i>Britholite</i> PQ12	<i>Apatite</i> PQ12
SiO <sub>2</sub> (wt. %)	29.52	29.33	48.20	48.34	43.84	34.20	33.76	19.42	1.09
TiO <sub>2</sub>	30.91	31.84	0.41	0.15	0.13	8.87	8.71	-	-
Al <sub>2</sub> O <sub>3</sub>	0.67	1.38	0.20	0.17	0.08	1.61	1.54	0.07	0.05
FeO	3.23	2.29	4.27	4.82	2.58	21.96	10.25	-	0.13
MnO	0.36	0.25	5.38	5.53	6.29	13.32	25.82	-	-
MgO	-	-	-	-	0.05	1.04	0.41	-	-
CaO	25.54	27.59	9.58	9.74	8.34	1.57	1.59	10.55	46.96
Na <sub>2</sub> O	0.32	0.48	12.69	12.69	11.18	2.81	2.55	0.24	0.43
K <sub>2</sub> O	-	-	0.35	0.22	0.33	6.08	6.05	-	-
P <sub>2</sub> O <sub>5</sub>	-	-	-	-	-	-	-	3.12	39.69
SrO	-	-	0.23	0.52	2.92	0.54	1.53	2.92	5.83
ZrO <sub>2</sub>	0.85	0.93	12.28	11.64	10.85	3.75	5.00	-	-
Y <sub>2</sub> O <sub>3</sub>	-	-	-	-	-	-	-	0.52	-
Nb <sub>2</sub> O <sub>5</sub>	3.51	2.80	0.52	0.95	2.10	1.40	0.11	-	-
La <sub>2</sub> O <sub>3</sub>	-	-	1.66	1.35	3.49	-	-	30.03	3.06
Ce <sub>2</sub> O <sub>3</sub>	1.02	-	2.11	1.83	3.87	-	-	29.93	3.00
Nd <sub>2</sub> O <sub>3</sub>	1.51	0.15	0.15	0.17	-	-	-	1.48	0.24
Sm <sub>2</sub> O <sub>3</sub>	0.56	-	-	0.46	-	-	-	-	-
PbO	-	-	-	-	0.33	-	-	-	-
ThO <sub>2</sub>	-	-	-	-	-	-	-	2.06	0.05
UO <sub>2</sub>	-	-	-	-	0.45	-	-	-	-
F <sup>-</sup>	-	1.64	-	-	2.05	2.73	1.90	1.41	3.68
Cl <sup>-</sup>	-	-	0.98	0.79	-	-	-	-	0.04
<i>Sum</i>	97.99	98.68	99.03	99.36	99.29	99.89	99.21	101.74	104.25
							O=(F <sup>-</sup> , Cl <sup>-</sup> )	0.59	1.56
							<i>Sum</i>	101.14	102.70
ΣREE <sub>2</sub> O <sub>3</sub>	3.09	0.15	3.93	3.82	7.36	-	-	61.44	6.30
n.Oxygens	5	5	73	73	78	31	31	26	26
Formula									
Si ( <i>apfu</i> )	1.03	1.01	24.58	24.58	24.80	7.67	7.79	<i>A site</i>	
Ti	0.81	0.82	0.16	0.06	0.06	1.50	1.51	Ca	3.07
Al	0.03	0.06	0.12	0.10	0.05	0.64	0.63	Sr	0.46
Fe <sup>2+</sup>	0.09	0.07	1.82	2.05	1.22	4.12	1.98	La	3.01
Mn	0.01	0.01	2.33	2.38	3.01	2.53	5.05	Ce	2.97
Mg	-	-	-	-	0.04	0.35	0.14	Nd	0.14
Ca	0.95	1.02	5.23	5.30	5.05	0.38	0.39	Fe	-
Na	0.02	0.03	12.55	12.51	12.26	1.22	1.14	Al	0.02
K	-	-	0.23	0.14	0.24	1.74	1.78	Na	0.12
Sr	-	-	0.07	0.15	0.96	0.07	0.21	Y	0.07
Zr	0.01	0.02	3.05	2.89	2.99	0.41	0.56	Th	0.13
Nb	0.06	0.04	0.12	0.22	0.54	0.14	0.01	<i>Sum</i>	10
La	-	-	0.31	0.25	0.73	-	-		
Ce	0.01	-	0.39	0.34	0.80	-	-	<i>T site</i>	
Nd	0.02	-	0.03	0.03	-	-	-	Si	5.28
Sm	0.01	-	-	0.08	-	-	-	P	0.72
Pb	-	-	-	-	0.05	-	-	<i>Sum</i>	6
Th	-	-	-	-	-	-	-		
U	-	-	-	-	0.05	-	-	F	1.18
F <sup>-</sup>	-	0.18	-	-	1.83	1.94	1.38	Cl	-
Cl <sup>-</sup>	-	-	0.85	0.68	-	-	-	OH	0.82
<i>Sum</i>	3.0	3.3	51.8	51.8	54.7	22.7	22.6	<i>Sum</i>	2

TABLE 3. Representative compositions of F-disilicates. Cations are listed following site occupancy, according to their formula.

	<i>Rinkite</i>		<i>Rosenbuschite</i>		<i>Hjordahlite</i>		<i>Wöhlerite</i>		<i>Lävenite</i>		<i>Mn-bearing lävenite</i>						
	PQ68	PQ39	PQ39	PQ42	PQ12C	PQ40A	PQ12C	PQ41	PQ42	PQ39	PQ12	PQ12					
SiO <sub>2</sub> (wt. %)	31.27	29.52	31.45	31.58	29.58	30.32	29.03	29.85	31.12	30.66	29.92	29.51					
TiO <sub>2</sub>	8.46	8.40	8.56	8.08	0.96	1.02	1.81	0.80	8.43	9.26	4.27	2.00					
Al <sub>2</sub> O <sub>3</sub>	0.32	-	0.08	0.05	0.08	-	-	0.51	0.09	-	-	0.17					
FeO	0.47	0.63	1.22	0.62	1.32	1.22	1.10	0.54	4.08	5.49	2.66	2.24					
MnO	0.69	0.58	4.56	3.75	3.74	2.83	4.47	4.85	9.66	8.46	11.40	12.66					
MgO	-	-	-	0.12	0.19	-	0.64	0.15	0.17	0.16	0.11	0.10					
CaO	27.51	27.66	24.08	24.09	30.46	31.52	26.23	25.67	13.27	14.54	2.59	4.94					
Na <sub>2</sub> O	8.36	8.59	10.62	10.86	6.80	7.10	7.44	7.88	10.18	10.55	12.35	11.51					
SrO	-	-	0.44	0.45	0.71	0.11	0.95	0.69	0.88	0.53	0.62	-					
ZrO <sub>2</sub>	-	0.37	12.11	14.75	15.96	17.09	13.98	14.12	16.50	14.41	26.10	31.59					
Nb <sub>2</sub> O <sub>5</sub>	-	0.42	0.97	0.58	1.66	2.15	9.25	12.83	2.88	2.78	9.66	1.34					
La <sub>2</sub> O <sub>3</sub>	5.42	5.39	0.42	0.36	0.33	0.47	-	-	-	-	0.16	0.61					
Ce <sub>2</sub> O <sub>3</sub>	9.49	10.02	0.26	0.38	0.87	0.46	-	0.05	0.06	-	-	1.02					
Nd <sub>2</sub> O <sub>3</sub>	3.21	3.04	-	0.42	0.14	-	0.34	-	-	-	-	0.48					
Sm <sub>2</sub> O <sub>3</sub>	0.35	-	-	-	0.41	-	-	0.09	-	0.13	0.11	-					
ThO <sub>2</sub>	0.11	-	-	-	0.03	-	0.11	0.05	-	0.09	-	0.56					
UO <sub>2</sub>	-	0.55	-	-	0.04	0.2	0.12	0.11	-	-	-	0.61					
F <sup>-</sup>	5.00	7.15	8.12	7.22	6.94	7.32	4.67	4.43	5.36	6.64	1.79	2.58					
<i>Sum</i>	100.6	102.30	102.9	103.31	100.2	101.8	100.1	102.62	102.7	103.70	101.7	101.91					
O=F <sup>-</sup>	2.10	3.01	3.42	3.04	2.92	3.08	1.97	1.87	2.26	2.80	0.75	1.09					
<i>Sum</i>	98.5	99.3	99.5	100.3	97.3	98.8	98.2	100.8	100.4	100.9	101.0	100.83					
$\Sigma \text{REE}_2\text{O}_3$	18.46	18.44	0.67	1.16	1.75	0.94	0.34	0.14	0.06	0.13	0.27	2.11					
Cations per 8 silicon atoms (apfu)																	
Na	2	2	Ca	6.54	6.53	Ca	8.52	8.47	Ca	0.71	-	Ca	2.81	2.57	Na	6.40	6.01
			Na	5.22	5.33	Na	3.56	3.63	Na	3.97	4.01	Na	5.06	5.34	Ca	0.74	1.43
Na	2.10	2.51	Sr	0.07	0.07	Sr	0.11	0.02	Sr	0.15	0.11	Sr	0.13	0.08	Sr	0.10	-
Ca	1.90	1.49	La	0.04	0.03	La	0.03	0.05	La	-	-	La	-	-	La	0.02	0.06
<i>Sum</i>	4	4	Ce	0.02	0.04	Ce	0.09	0.04	Ce	-	0.005	Ce	0.01	-	Ce	-	0.10
			Nd	-	0.04	Nd	0.01	-	Nd	0.03	-	Nd	-	-	Nd	-	0.05
Ca	5.55	6.54	Sm	-	-	Sm	0.04	-	Sm	-	0.01	Sm	-	0.01	Sm	0.01	-
La	0.51	0.54	<i>Sum</i>	12	12	<i>Sum</i>	12	12	<i>Sum</i>	5	4	<i>Sum</i>	8	8	Nb	0.65	-
Ce	0.88	0.99										<i>Sum</i>	8	7.6			
Nd	0.29	0.29	Ti	1.63	1.54	Ti	0.19	0.20	Ca	7.03	7.23	Mn	2.10	1.87			
Sm	0.03	-	Fe	0.26	0.13	Fe	0.30	0.27	Fe	0.25	0.12	Fe	0.87	1.20	Mn	2.58	2.89
<i>Sum</i>	7	8	Mn	0.98	0.80	Mn	0.85	0.63	Mg	0.26	0.06	Ti	0.02	0.00	Fe	0.60	0.50
Ti	1.61	1.71	Zr	1.50	1.82	Zr	2.10	2.20	<i>Sum</i>	8	8	Mg	0.07	0.06	Ti	0.26	0.41
Fe	0.10	0.14	Nb	0.11	0.07	Nb	0.20	0.26	<i>Sum</i>	4	4	Ca	0.84	1.50	Mg	0.05	0.04
Mn	0.15	0.13	<i>Sum</i>	4	4	Ca	0.28	0.44	Zr	1.88	1.81	<i>Sum</i>	4	4.6	Nb	0.52	0.16
Mg	-	-				<i>Sum</i>	4	4	Ti	0.37	0.16	Zr	2.06	1.83	<i>Sum</i>	4	4
Zr	-	0.05							Nb	1.15	1.52	Ti	1.61	1.82	Zr	3.40	4.15
Nb	-	0.05							Mn	0.59	0.51	Nb	0.33	0.33	Ti	0.60	-
<i>Sum</i>	2	2							<i>Sum</i>	4	4	<i>Sum</i>	4	4	Nb	-	4.1
Si	7.90	8.00	Si	7.98	7.99	Si	7.97	8.00	Si	8.00	7.84	Si	7.97	8.00	Si	8.00	7.95
Al	0.10	-	Al	0.02	0.01	Al	0.03	-	Al	-	0.16	Al	0.03	-	Al	-	0.05
O	28	28	O	28	28	O	28	28	O	28	28	O	28	28	O	28	28
F	4	4															
O	3.95	2.39	O	2.08	2.67	O, OH	2.56	2.42	O, OH	4.24	4.51	O, OH	3.88	3.02	O, OH	6.50	5.80
F	4.05	5.61	F	5.92	5.33	F	5.44	5.58	F	3.76	3.49	F	4.12	4.98	F	1.50	2.20
<i>Sum</i>	8	8	<i>Sum</i>	8	8	<i>Sum</i>	8	8	<i>Sum</i>	8	8	<i>Sum</i>	8	8	<i>Sum</i>	8	8